

NOTE TO USERS

This reproduction is the best copy available.

UMI[®]

Symplectic Integration of Simple Collisions: A Backward Error Analysis

David Cottrell

Department of Mathematics and Statistics,

McGill University, Montréal

Québec, Canada

June, 2004

A thesis submitted to the Faculty of Graduate Studies and Research
in partial fulfillment of the requirements of the degree of
Master of Science

Copyright © David Cottrell, 2004



Library and
Archives Canada

Bibliothèque et
Archives Canada

Published Heritage
Branch

Direction du
Patrimoine de l'édition

395 Wellington Street
Ottawa ON K1A 0N4
Canada

395, rue Wellington
Ottawa ON K1A 0N4
Canada

Your file *Votre référence*

ISBN: 0-494-06385-8

Our file *Notre référence*

ISBN: 0-494-06385-8

NOTICE:

The author has granted a non-exclusive license allowing Library and Archives Canada to reproduce, publish, archive, preserve, conserve, communicate to the public by telecommunication or on the Internet, loan, distribute and sell theses worldwide, for commercial or non-commercial purposes, in microform, paper, electronic and/or any other formats.

The author retains copyright ownership and moral rights in this thesis. Neither the thesis nor substantial extracts from it may be printed or otherwise reproduced without the author's permission.

AVIS:

L'auteur a accordé une licence non exclusive permettant à la Bibliothèque et Archives Canada de reproduire, publier, archiver, sauvegarder, conserver, transmettre au public par télécommunication ou par l'Internet, prêter, distribuer et vendre des thèses partout dans le monde, à des fins commerciales ou autres, sur support microforme, papier, électronique et/ou autres formats.

L'auteur conserve la propriété du droit d'auteur et des droits moraux qui protègent cette thèse. Ni la thèse ni des extraits substantiels de celle-ci ne doivent être imprimés ou autrement reproduits sans son autorisation.

In compliance with the Canadian Privacy Act some supporting forms may have been removed from this thesis.

Conformément à la loi canadienne sur la protection de la vie privée, quelques formulaires secondaires ont été enlevés de cette thèse.

While these forms may be included in the document page count, their removal does not represent any loss of content from the thesis.

Bien que ces formulaires aient inclus dans la pagination, il n'y aura aucun contenu manquant.


Canada

Abstract

Molecular Dynamics simulations often involve the numerical integration of pair-wise particle interactions with a constant step size method. Of primary concern in these simulations is the introduction of error in velocity statistics. We consider the simple example of the symplectic Euler method applied to two-particle collisions in one dimension governed by linear restoring force and use backward error analysis to predict these errors. For nearly all choices of system and method parameters, the post-collision energy is not conserved and depends upon the initial conditions of the particles and the step size of the method. The analysis of individual collisions is extended to predict energy growth in systems of particles in one dimension.

Résumé

Les simulations de dynamique moléculaire impliquent souvent l'intégration numérique d'interactions entre des paires de particules avec une méthode à pas de temps constant. Une considération importante de ces simulations est l'introduction d'erreur dans les statistiques de vitesse. Nous considérons l'exemple simple de la méthode d'Euler symplectique appliquée aux collisions de deux particules en une dimension gouvernées par une force de restauration linéaire, et nous utilisons l'analyse d'erreur implicite (backward error analysis) pour prédire ces erreurs. Pour la plupart des choix de paramètres de système et de méthode, l'énergie post-collision n'est pas préservée et dépend des conditions initiales des particules et du pas de temps de la méthode. On étend l'analyse des collisions individuelles à la prédiction de la croissance d'énergie dans les systèmes de particules en une dimension.

Acknowledgements

Firstly I thank my supervisor, Paul Tupper, for introducing this project to me and for guiding me so patiently and subtly throughout the work. I am indebted to him for his time and enthusiasm which gave me both direction and motivation throughout the course of this research. His diverse interests have provided opportunities for learning well beyond the scope of this project.

I cannot deny myself the pleasure of publicly thanking Nilima Nigam and the attendees of the McGill Applied Math seminar (CAMPY) for their open ears and thoughtful minds. The seminars offered a casual and friendly atmosphere which allowed me to test my own presentations for clarity and accuracy and at the same time gave me the opportunity to encounter a wide range of interesting problems in applied mathematics.

I finally thank my parents for their support, energy and their diligent proof-reading.

Table of Contents

Abstract	i
Résumé	iii
Acknowledgements	v
Introduction	1
1 Symplectic Integration	3
2 Modified Equations & Backward Error Analysis	9
2.1 Construction of the modified equation	12
2.2 Modified equations of linear systems	16
2.2.1 Damped oscillator with symplectic Euler	16
2.2.2 Undamped oscillator with symplectic Euler	23
3 Numerical Approximation of a Simple Collision	31
3.1 Error due to particle-wall collisions	32
3.1.1 Damped linear-spring collision with the symplectic Euler method	35
3.1.2 Undamped linear-spring collision with the symplectic Euler method	38
4 Systems of Particles: Energy Growth in One-Dimensional Systems	51

4.1	Two-particle collisions	52
4.2	Systems of particles	54
4.2.1	Consideration of dimension	55
4.2.2	Energy growth for 1-d system	55
	Conclusion	69
	A Glossary of symbols	71

Introduction

In the field of molecular dynamics, numerical simulations are commonly used to obtain approximate solutions to the systems of ordinary differential equations defining the dynamics of interacting particles. In many situations, the differential equations are integrated over very long periods of time with relatively large fixed time-steps. Though the trajectories of the computed solutions in these cases may diverge from those of the true solution, it is believed that the simulations can well approximate many important system statistics. Yet it has been shown [53] that certain methods, such as step-and-project methods, while exactly conserving energy, can yield incorrect statistics. There is evidence that symplectic methods tend to provide relatively unbiased statistics. However, the introduction of unbounded energy growth or “intrinsic” (anti)damping in some conservative systems by symplectic methods raises questions regarding the interpretation of these computed systems.

The goal of this work is to investigate the introduction of errors by fixed time-step integrators applied to systems of locally interacting particles. The approach shown here also provides a framework for improving or constructing methods which will provide more dependable and more desirable results. Though the presentation revolves around a specific problem, the methods are in many cases relevant to other problems in computational molecular or gas dynamics.

Chapter 1

Symplectic Integration

Symplecticity, as it applies to numerical methods, to a large extent stems from considering the qualities of generating functions for Hamiltonian systems. The reader is referred to [24] for a brief overview of generating functions for Hamiltonian systems. Since Hamiltonian flow is characterized by a generating function of a certain form (and vice versa), it is reasonable to consider numerical methods based on such mappings. Loosely speaking, methods which conserve Hamiltonian structure are called symplectic. Given an autonomous Hamiltonian system

$$\dot{p} = -\nabla_q \mathcal{H}(p, q), \quad \dot{q} = \nabla_p \mathcal{H}(p, q).$$

the flow is given by

$$\begin{pmatrix} q(t + \tau) \\ p(t + \tau) \end{pmatrix} = \varphi_\tau(q(t), p(t)) \tag{1.1}$$

where the flow operator, φ_τ , must satisfy

$$(\nabla \varphi_\tau)^T \mathbf{J} (\nabla \varphi_\tau) = \mathbf{J}, \quad \mathbf{J} = \begin{pmatrix} \mathbf{0} & \mathbf{I} \\ -\mathbf{I} & \mathbf{0} \end{pmatrix}. \tag{1.2}$$

We say that a one step method

$$\begin{pmatrix} q_{n+1} \\ p_{n+1} \end{pmatrix} = \Phi_h(q_n, p_n) \quad (1.3)$$

is symplectic if the numerical flow map, Φ_h , satisfies (1.2). This statement of symplecticity is very similar to that concerning the orthogonality of the matrix $\nabla\Phi_h$ (consider (1.2) with \mathbf{J} replaced by the identity), where instead of conservation of lengths of vectors in the phase space, we now have conservation of the magnitude of oriented areas. It is important to note that in contrast to the generating functions from which they are derived, symplectic methods conserve Hamiltonian structure but do not, except for trivial cases, conserve the value of the original Hamiltonian.

The notion of symplecticity was first put forth by Weyl in 1939 [59]. The word is taken from the greek adjective and loosely means “plaited together” as it is used in anatomy to describe certain bone structures. The connection between Hamiltonian systems and symplecticity motivated the development of symplectic integrators for Hamiltonian systems. De Vogelaere [10] initiated this development around 1956 but it was not until the 1980’s that the area of symplectic integration was to experience substantial growth under a theoretically rigorous framework. Through the eighties and early nineties, the foundations of the subject were developed in the work of Ruth [42], Channell [6], Menyuk [36], Neishtadt [38], Feng [13], Lasagni [32], Suris [51], Channell and Scovel [7], and Sanz-Serna [44] among others, many of whom were concurrently developing complimentary ideas in modified equations and backward error analysis. During this period there was also much activity in the analysis and understanding of symplectic methods in applications. Fast explicit symplectic algorithms for separable Hamiltonians (e.g. in molecular dynamics) [5], methods for rigid multi-body systems [2] and symplectic variable step size integrators [24] [50] were developed. The explosion of research in symplectic integration has left many open and fairly accessible problems. McLachlan and Scovel’s survey of open problems [34], valid as of

1998, provides an excellent overview of some of these unanswered questions.

Sanz-Serna describes two kinds of symplectic methods, differentiating between those methods which have a history in other fields and “just happen” to be symplectic and those which are derived from generating functions, constructed especially for Hamiltonian systems [44]. This distinction, however, is purely historical. The structure preserving nature of these methods explains the surprisingly good behaviour of many simple, low-order symplectic methods as compared with higher order non-symplectic methods such as multistep methods, which cannot be symplectic [52], [21]. A rigorous explanation of this phenomenon lies in backward error analysis. Some of the main results of this analysis for symplectic integrators are presented here while an introduction to backward error analysis will be given in the Chapter 2.

Probably the most important result concerning the behaviour of symplectic methods applied to Hamiltonian problems is that of their long-time near energy preservation. One of the earliest results comes from Neishtadt [38] who shows that if the perturbation to the Hamiltonian due to the integrator is of size ϵ , then the energy will be $\mathcal{O}(\epsilon)$ close to the true energy over time intervals of order $\mathcal{O}(e^{c/\epsilon})$. Later, under the structure of backward error analysis, more detailed results involving the trajectories of numerical solutions were presented by Sanz-Serna [44], Benettin and Giorgilli [3], Hairer [20], Hairer and Lubich [22], and Reich [41]. It was shown that for symplectic methods applied to Hamiltonian systems, the numerical solution is very near the exact solution of a nearby Hamiltonian over time intervals $\mathcal{O}(1/h)$. Skeel [49] notes that, though the time $\mathcal{O}(1/h)$ is theoretically large, in practice it can be much shorter than the interval of integration. The fact that there is little evidence of poor energy conservation after such a time length suggests that it may be possible to extend the backward error analysis to much longer time scales.

This excellent behaviour is often limited to step sizes below a critical number, above which the behaviour of solutions suddenly worsens, sometimes even leading to

energy blowing up in finite time (i.e. over-flow in actual computations) [48]. Furthermore, symplecticity in some sense is an indication of error. For Hamiltonian systems with no other first integrals. Ge and Marsden [65] show that the energy cannot be conserved by a symplectic integrator except in trivial cases where the numerical and analytic trajectories agree up to a reparameterization of time. So the excellent long-term behaviour of symplectic methods is somewhat surprising. This does, however, raise the question of whether the long-term or infinite time behaviour in floating point arithmetic is the same as, or at least resembles, the behaviour in infinite-precision calculations. The effect of rounding errors on symplectic methods has been considered by [11], [49] and [45], among others, but the effect of such errors on infinite-time behaviour remains, to a large extent, an open problem.

There are several other side benefits of using symplectic schemes in long-time integration. KAM theory implies that symplectic integrators may have enhanced non-linear stability [43]. Volume preservation in phase space is a trivial consequence of symplecticity. Methods which are both volume preserving and reversible, conserve detailed balance [35] – that is they conserve equilibrium conditions.

The symplectic method of interest here is symplectic Euler I, as it is termed in [25]:

$$\text{Symplectic Euler I} \begin{cases} q_{n+\frac{1}{2}} &= q_n + \frac{h}{2} \nabla_p \mathcal{H}(p_{n+\frac{1}{2}}, q_n) \\ p_{n+\frac{1}{2}} &= p_n - \frac{h}{2} \nabla_q \mathcal{H}(p_{n+\frac{1}{2}}, q_n) \end{cases}$$

When composed with its adjoint,

$$\text{Symplectic Euler II} \begin{cases} q_{n+\frac{1}{2}} &= q_n + \frac{h}{2} \nabla_p \mathcal{H}(p_n, q_{n+\frac{1}{2}}) \\ p_{n+\frac{1}{2}} &= p_n - \frac{h}{2} \nabla_q \mathcal{H}(p_n, q_{n+\frac{1}{2}}) \end{cases}$$

and applied to a separable Hamiltonian system (i.e. $\mathcal{H}(p, q) = T(p) + V(q)$), the

famous Störmer-Verlet or leapfrog method is obtained:

$$\text{Störmer-Verlet} \begin{cases} q_{n+1} &= q_n + hT'(p_{n+\frac{1}{2}}) \\ p_{n+\frac{1}{2}} &= p_{n-\frac{1}{2}} - hV'(q_n) \end{cases}. \quad (1.4)$$

If the symplectic Euler method (I or II) is applied to a system with a separable Hamiltonian, an explicit representation can easily be obtained

$$\text{SE I} \begin{cases} q_{n+\frac{1}{2}} &= q_n + \frac{h}{2}T'(p_{n+\frac{1}{2}}) = q_n + \frac{h}{2}T'(p_n - \frac{h}{2}V'(q_n)) \\ p_{n+\frac{1}{2}} &= p_n - \frac{h}{2}V'(q_n) \end{cases}. \quad (1.5)$$

The method, as written in (1.5) but with time-steps of length h , applied to a particularly simple but illustrative problem will be the subject of the analysis in the rest of this work.

The Störmer-Verlet method is very similar to the symplectic Euler method above. Many of the results presented here for the symplectic Euler method will also hold true for the Störmer-Verlet method. To illustrate the similarity of the two methods for certain problems, we consider the one-step formulation of the Störmer-Verlet method (1.4). If we apply the symplectic Euler I method (1.5) with time-step $2h$ and the Störmer-Verlet method (1.4) with time-step h to a separable Hamiltonian problem with $T(p) = \frac{1}{2}|p|^2$ and initial conditions $\bar{p}_{-\frac{1}{2}} = p_0 = p^0$, $\bar{q}_0 = q_0 = q^0$ then we have

Störmer-Verlet (h)	SE I ($2h$)
$\bar{q}_1 = \bar{q}^0 + h\bar{p}_{\frac{1}{2}}$	$q_{\frac{1}{2}} = q^0 + hp_{\frac{1}{2}}$
$\bar{p}_{\frac{1}{2}} = \bar{p}^0 - hV'(\bar{q}^0)$	$p_{\frac{1}{2}} = p^0 - hV'(q^0)$
$\bar{q}_2 = \bar{q}_1 + h\bar{p}_{1+\frac{1}{2}}$	$q_1 = q_{\frac{1}{2}} + hp_1$
$\bar{p}_{1+\frac{1}{2}} = \bar{p}_{\frac{1}{2}} - hV'(\bar{q}_1)$	$p_1 = p_{\frac{1}{2}} - hV'(q_{\frac{1}{2}})$

where the bars merely indicate the difference between the solutions from the two methods. We can see that, for the first two steps, the methods produce the same iterates if we consider the transformation $\bar{q}_i \rightarrow q_{\frac{i}{2}}$, $\bar{p}_{i-\frac{1}{2}} \rightarrow p_{\frac{i}{2}}$, $i = 1, 2, \dots$, mapping the sequence of steps given by the Störmer-Verlet method to that given by the

symplectic Euler method. It is evident that the first two steps are equivalent under this transformation and it is possible to show by induction that this is true for all steps. For this particular problem, with constant velocity initial conditions, the two methods give rise to the same iterates and the results for the symplectic Euler method presented in the preceding chapters also hold for the Störmer-Verlet method.

Chapter 2

Modified Equations & Backward Error Analysis

“Divergent series are the invention of the devil, and it is shameful to base on them any demonstration whatsoever.” - Abel, 1828

The idea of modified equations is to describe a numerical solution as points along the exact solution of a modified problem which is in some sense near the original problem. That is, the *exact* solutions of the modified problem “interpolate” the numerically approximated solution. The word interpolate is used loosely, and should be thought of as meaning merely that for a given fixed time step, h , the modified solution passes through the points of the numerical solution. For large h , the modified solutions may vary wildly between points of the numerical solution and do not necessarily provide a good or natural interpolant to the numerical solution in the traditional sense.

Though notions of backward analysis and backward stability of problems has been around for some time, the method of modified equations as a means of (backward) analyzing numerical solutions of differential equations is a much more recent development. The general concept of backward error analysis was developed and used

extensively by Wilkinson in his work during the 1950s and 1960s, primarily in the field of numerical linear algebra [62], [61]. N. Higham [28] notes that von Neumann and Goldstine [58] as well as Turing [56] made implicit use of backward error ideas several years earlier. The method of modified equations has existed under various names such as equivalent equations, truncation error methods, augmented systems and differential approximations. Early ideas of modified equations can be traced back to the 1960's in the works of Dally [9], Noh and Protter [39], Moser [37], Hirt [29] and Yanenko and Shokin [63], though in many cases the modified equations or modified solutions were not explicitly tied to numerical methods. Despite these relatively early beginnings, it was not until around 1990 that a rigorous formulation of the subject was penned, in many cases as a result of investigations of the long-term behaviour of symplectic integrators. The papers by Griffiths and Sanz-Serna [19], Feng [14], Sanz-Serna [44], McLachlan and Atela [33], Yoshida [64] and Eirola [12] set down the theoretical foundations of the subject and started a flurry of activity in the fields of modified equations and geometric numerical integration. Interestingly, the problem of interpolating discrete dynamical systems using formal series received a much earlier treatment in the context of combinatorics by G. Labelle [30] in 1980. It seems that the development of the theory of backward error analysis for numerical integration occurred independently with the only reference to Labelle coming from Corless [8] in 1994.

The primary motivation for seeking such modified problems is that frequently they are easier to understand than the discrete dynamical systems (i.e. difference equations) which define the numerical integrator. In essence, they are useful because models are usually developed and expressed in terms of continuous systems which are difficult to compare with discrete maps. However, modified equations can also prove useful in obtaining long-term estimates of quantities defined strictly by discrete models with maps sufficiently close to the identity.

Furthermore, the practical construction of these modified problems allows for new consideration of conditioning and stiffness of problems. Corless points to the idea of a measurable statistic being “well-enough conditioned” – “if the relevant statistic is insensitive to perturbations of the problem” [8] – and contrasts this to the traditional idea of “well conditioned” which is associated with stability under perturbations of the initial data. Corless also contemplates an alternative definition of stiff and chaotic problems. He defines a chaotic problem as “one where a solution with good backward error may be easily computed with explicit methods while a solution with good forward error is too expensive” and “a stiff problem is one where a solution with good forward error is easily computed using implicit methods, while a solution with good backward error is too expensive” [8]. He further notes that these ideas are qualitative, that there exists a spectrum of problems with aspects of both properties.

Backward error analysis has a history of succeeding where forward analysis fails. Wilkinson’s classical result regarding the stability of Gaussian elimination [60] could not be explained through the traditional forward analysis approach. Modified equations have been used to explain the success of numerical methods applied to chaotic systems [8] and perhaps most notably they have been used to prove a series of theorems regarding the structure preservation of certain types of methods (e.g. energy conservation of symplectic methods). Briefly, these theorems are of the form, “if the system is Hamiltonian and the method is symplectic, then the modified system is also Hamiltonian”. A similar statement holds with Hamiltonian and symplectic replaced by reversible and symmetric respectively. The proof of these statements is by induction and can be found in [25], [26], [23] and [20], but was first given by Benettin and Giorgilli [3]. These results are closely related to the structural properties of certain subspaces of the infinite-dimensional Lie algebra of smooth vector fields on \mathbb{R}^p . However, structural properties shared by the numerical methods and the original system

are not in general inherited by the modified equation. A simple counter-example of a system and method which share a structural property but give rise to modified equations which do not possess the same property can be found in [18].

There are two other approaches which fall under the scope of backward error analysis of numerical integrators and should be briefly mentioned: shadowing and asymptotic expansion. In shadowing, one does not seek a modified problem but keeps the equation fixed and changes the initial conditions. In backward error analysis both are allowed to change [8]. The method of asymptotic expansion is quite similar to that of modified equations. Instead of expanding the modified equation in powers of h , one expands the modified solution \tilde{y} . This approach, termed asymptotic expansion in [23], leads to distinctly different and less desirable results. In particular, asymptotic expansions are more sensitive to truncation than backward analysis. The truncation error grows linearly in time for backward error analysis (modified equations) and polynomial in time for asymptotic expansions [23]. Furthermore there are many other good properties of the modified equations which the asymptotic expansions do not possess: the semigroup property ($\tilde{y}_N(t+s, y_0) = \tilde{y}_N(t, \tilde{y}(s, y_0))$), the structure property (e.g. symplectic method + Hamiltonian system gives Hamiltonian modified equation) and error estimates with exponentially small error [23].

2.1 Construction of the modified equation

Consider the system of ordinary differential equations

$$\dot{y} = f(y) \tag{2.1}$$

and apply the numerical method Φ_h to (2.1) to obtain a numerical approximation

$$y_{n+1} = \Phi_h(y_n). \tag{2.2}$$

We seek a perturbed or modified function f_h such that the solution, \tilde{y} , of

$$\dot{\tilde{y}} = f_h(\tilde{y}) \quad (2.3)$$

matches the solution of (2.2) at the points $t = 0, h, 2h, \dots$.

In general, it is not possible to obtain an expression for f_h explicitly. Instead f_h can be written as a formal series in powers of h , with the terms defined recursively. This series does not converge in general but suitable truncations of the series can approximate f_h well. There are several approaches to calculating the terms in the h -expansion of f_h . Here we closely follow the approach of Hairer et al. [24]. The idea is to take expansions of \tilde{y} and Φ_h and match terms of equal powers of h . We start by writing f_h as a series in h .

$$f_h = f + hf_2 + h^2f_3 + h^3f_4 + \dots \quad (2.4)$$

The modified solution can now be written as

$$\begin{aligned} \tilde{y}(t+h) &= \tilde{y} + h\dot{\tilde{y}} + \frac{h^2}{2!}\tilde{y}^{(2)} + \frac{h^3}{3!}\tilde{y}^{(3)} + \dots \\ &= \tilde{y} + hf_h + \frac{h^2}{2!}f'_hf_h + \frac{h^3}{3!}(f''_h(f_h, f_h) + f'_hf'_hf_h) \\ &= \tilde{y} + h(f + hf_2 + h^2f_3 + \dots) \\ &\quad + \frac{h^2}{2!}(f' + hf'_2 + h^2f'_3 + \dots)(f + hf_2 + h^2f_3 + \dots) \\ &\quad + \frac{h^3}{3!}((f'' + hf''_2 + h^2f''_3 + \dots)(f + hf_2 + h^2f_3 + \dots, f + hf_2 + h^2f_3 + \dots) \\ &\quad + (f' + hf'_2 + h^2f'_3 + \dots)(f' + hf'_2 + h^2f'_3 + \dots)(f + hf_2 + h^2f_3 + \dots)) \\ &\quad + \dots \\ &= \tilde{y} + hf + h^2(f_2 + \frac{1}{2!}f'f) + h^3(f_3 + \frac{1}{2!}f'_2f + \frac{1}{2!}f'f'_2 + \frac{1}{3!}f''ff) + \dots \end{aligned} \quad (2.5)$$

Here f, f', f'' represent $f(\tilde{y}), f'(\tilde{y}), f''(\tilde{y})$ respectively. Also note that f' is the Jacobian of f and $f'', f^{(3)}, \dots$ are binary, ternary, ... operators taking 2, 3, ... arguments.

Term by term comparison of (2.5) to the expansion of Φ_h ,

$$\Phi_h(y) = y + hf(h) + h^2d_2(y) + h^3d_3(y) + \dots$$

gives the functions f_{k+1} in terms of the f_2, f_3, \dots, f_k

$$f_2 = d_2 - \frac{f'f}{2!},$$

$$f_3 = d_3 - \frac{1}{2!}(f'f_2 + f'_2f) - \frac{1}{3!}(f''(f, f)). \text{ etc.}$$

Methods for implementing this recursion are given by Hairer [24] and by Ahmed and Corless [1], among others. For most functions f , the symbolic computations become very costly for higher order terms. An elegant representation of the recurrence relation can be achieved through the use of trees and ordered trees [27], [24], [31] but will not be presented here as it is outside the scope of this work.

In general, the series (2.4) diverges and the infinite order modified equation does not exist. W.J.Beyn [4] provides a simple yet illustrative example showing that it is in general not possible to embed an arbitrary discrete dynamical system into a continuous one. Nonetheless, taking a finite number of terms of the series (2.4) yields a truncated modified equation that can still provide a good approximation to the behaviour of the discrete dynamical system.

A very similar approach is taken by Reich [41] to develop an expression for the modified equation, the main difference there being that a recursive expression is written to define the terms f_2, f_3, \dots of the modified equation (i.e. f_{i+1} is defined in terms of f_i). The approach is exactly the same otherwise but may be advantageous in the practical construction of modified equations. With the development of symbolic computing packages such as Maple, the often cumbersome task of computing terms of the modified equation can be fully automated. There are several published codes for symbolically computing modified equations in Maple [24], [1].

There exist several statements concerning the nearness of solutions of the truncated modified equation to the numerical solution. The following statement is taken

directly from [23].

Proposition 2.1. *Exponentially small estimates. If the vector field $f(y)$ is real analytic and if the truncation index N is chosen as $N \approx \text{const}/h$ with a suitable constant, then it holds (with some $\gamma > 0$)*

$$y_N - \tilde{y}_N(h) = \mathcal{O}(e^{-\gamma/h})$$

Proofs of this and other related estimates can be found in [3], [22], [25] and [40].

Corless [8] provides a completely different approach for scalar problems which expresses the modified equation as an infinite formal product instead of an infinite formal series. The approach may provide more information about where (in phase space) the infinite order modified equation exists and can be determined. It also seems that while the analysis of higher dimensional problems may be more complicated than in the scalar case, even a partial description via this process may provide valuable information. Corless, however, indicates that in these more complicated systems his approach would probably not be helpful.

Instead of expanding (2.3) and (2.2) and matching terms, Corless considers differentiating (2.2) with respect to time and using (2.3) to express derivatives of the numerical solution in terms of the r.h.s. of the modified equation:

$$\begin{aligned} \dot{y}_{n+1} = \Phi'_h(y_n)\dot{y}_n &\Rightarrow f_h(y_{n+1}) = \Phi'_h(y_n)f_h(y_n) \\ &\Rightarrow f_h(\Phi_h(y_n)) = \Phi'_h(y_n)f_h(y_n). \end{aligned}$$

If $\Phi'_h(y)$ is invertible in some neighborhood of y and the discrete dynamical system (2.2) simple enough, the problem of finding the modified equation (in this limited region) can be transformed into the problem of finding a suitable collection of infinite products. In the example presented by Corless, the mapping $y_n \rightarrow \Phi_h(y_n)$ is inverted (so that it is a contraction) and the iteration is run backwards.

2.2 Modified equations of linear systems

For systems of linear ordinary differential equations with constant coefficients, the task of determining the modified equation is greatly simplified and a closed form expression of the modified equation can often be obtained. If the modified equation of a linear one-step method applied to a linear ordinary differential equation exists, then it is necessarily linear. This is illustrated by considering a linear system

$$\dot{y} = \mathbf{A}y. \quad (2.6)$$

and applying a one-step linear method which yields $\phi_h(y) = R(h\mathbf{A})y$. We then have that $\tilde{y}(nh) = y_n = R(h\mathbf{A})^n y_0$. Thus

$$\begin{aligned} \tilde{y}(t) &= R(h\mathbf{A})^{\frac{t}{h}} y_0 = \exp\left(\frac{t}{h} \ln(R(h\mathbf{A}))\right) y_0 \\ &\Rightarrow \boxed{\dot{\tilde{y}} = \frac{1}{h} \ln(R(h\mathbf{A})) \tilde{y}}. \end{aligned} \quad (2.7)$$

For a *consistent* one-step linear method, $R(h\mathbf{A}) = (\mathbf{I} + \mathbf{A}_h)$ for some matrix \mathbf{A}_h with $\mathbf{A}_h \rightarrow 0$ as $h \rightarrow 0$. In this case the existence of the modified equation corresponds to the matrix ln series being defined [24]. If \mathbf{A}_h is diagonalizable, we are guaranteed that $\ln(R(h\mathbf{A}))$ is well defined for sufficiently small h , taking the principal branch of the complex function in the case that $R(h\mathbf{A})$ has negative eigenvalues. The problem of finding the modified equation reduces to that of finding an eigenvalue-eigenvector decomposition of the matrix \mathbf{A}_h .

2.2.1 Damped oscillator with symplectic Euler

We now consider the damped oscillator with linear restoring force and the symplectic Euler method and seek the form of the modified equation. In the future, we will use the modified solution to obtain an analytic expression of the error induced when numerically integrating collisions between particles with linear restoring force. The

damped harmonic (linear) oscillator is given by

$$\ddot{x} + \gamma\dot{x} + kx = 0 \quad (2.8)$$

and can be written in first-order form.

$$\begin{pmatrix} \dot{x} \\ \dot{v} \end{pmatrix} = \begin{pmatrix} 0 & 1 \\ -k & -\gamma \end{pmatrix} \begin{pmatrix} x \\ v \end{pmatrix} \quad (2.9)$$

where x and v are the position and velocity of the point mass, $k > 0$ and γ are Young's modulus and viscosity per unit mass respectively. The dissipation during the collision is given by γ where $\gamma > 0$ and $\gamma < 0$ correspond to damped and anti-damped collisions respectively. The eigenvalues of the matrix appearing in (2.9) are

$$\lambda_{\pm}^{exact} = -\frac{\gamma}{2} \pm \sqrt{\gamma^2 - 4k}. \quad (2.10)$$

The arguments of the radical determine whether the system is under-damped ($\gamma^2 < 4k$), critically damped ($\gamma^2 = 4k$) or over-damped ($\gamma^2 > 4k$). Fig. 2.1 illustrates the three regions. In the application considered in Chapter 3, we wish to study problems where the mass returns to its rest position in finite time, thus we might consider restricting ourselves to the under-damped case where λ is complex (see Fig. 2.2). In more concrete terms, we want to limit our study to the cases where the oscillator does in fact oscillate. This is particularly important if the restoring force governing a collision between two bodies is modeled as a linear force with linear damping and if we wish to ensure that the collision is not completely inelastic. Care must be taken in doing this as the under-damped regions in the exact system and the modified system are not the same. To proceed, we must first determine the modified equation and then determine the behaviour of the modified eigenvalues through various regions of $(kh^2, \gamma h)$ parameter space. It will be seen that these dimensionless parameters determine the behaviour of the discrete and the modified system up to a rescaling of time. We begin by applying symplectic Euler to the problem at hand (2.9).

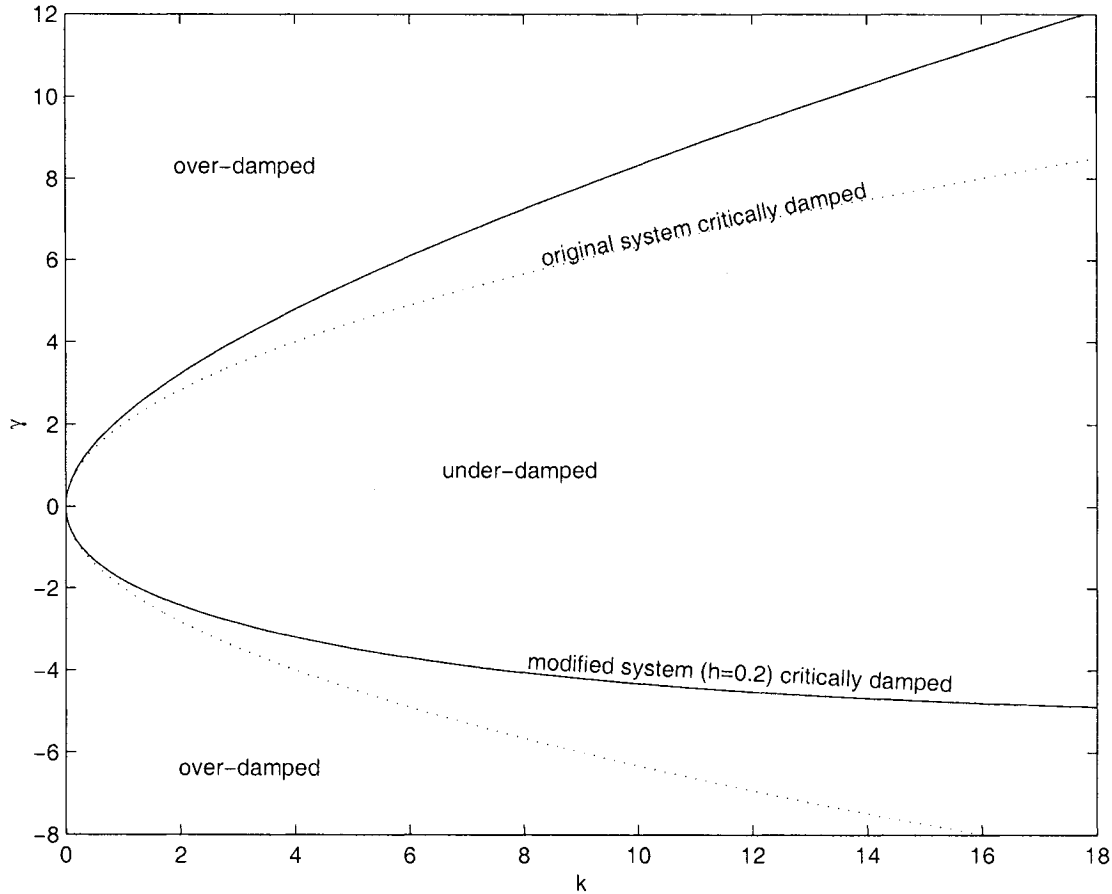


Figure 2.1: Regions of under- and over-damping for the original system (2.9) and the modified system (2.12) plotted in (k, γ) -parameter space. Here k and γ are the spring stiffness and damping parameters respectively. The behaviour of the original system and modified system is determined from the value of the eigenvalues λ_{\pm} (2.10) and $\tilde{\lambda}_{h\pm}$ (2.20) respectively.

Applying the symplectic Euler method (1.5) to (2.9) we obtain the explicit one-step map

$$y_{n+1} = \frac{1}{1 + \gamma h} (\mathbf{I} + \mathbf{A}_h) y_n, \quad \mathbf{A}_h = \begin{pmatrix} \gamma h - kh^2 & h \\ -kh & 0 \end{pmatrix} \quad (2.11)$$

where $\gamma h \neq -1$ and $(x_n, v_n)^T$ has been replaced with y_n for ease of notation. Notice

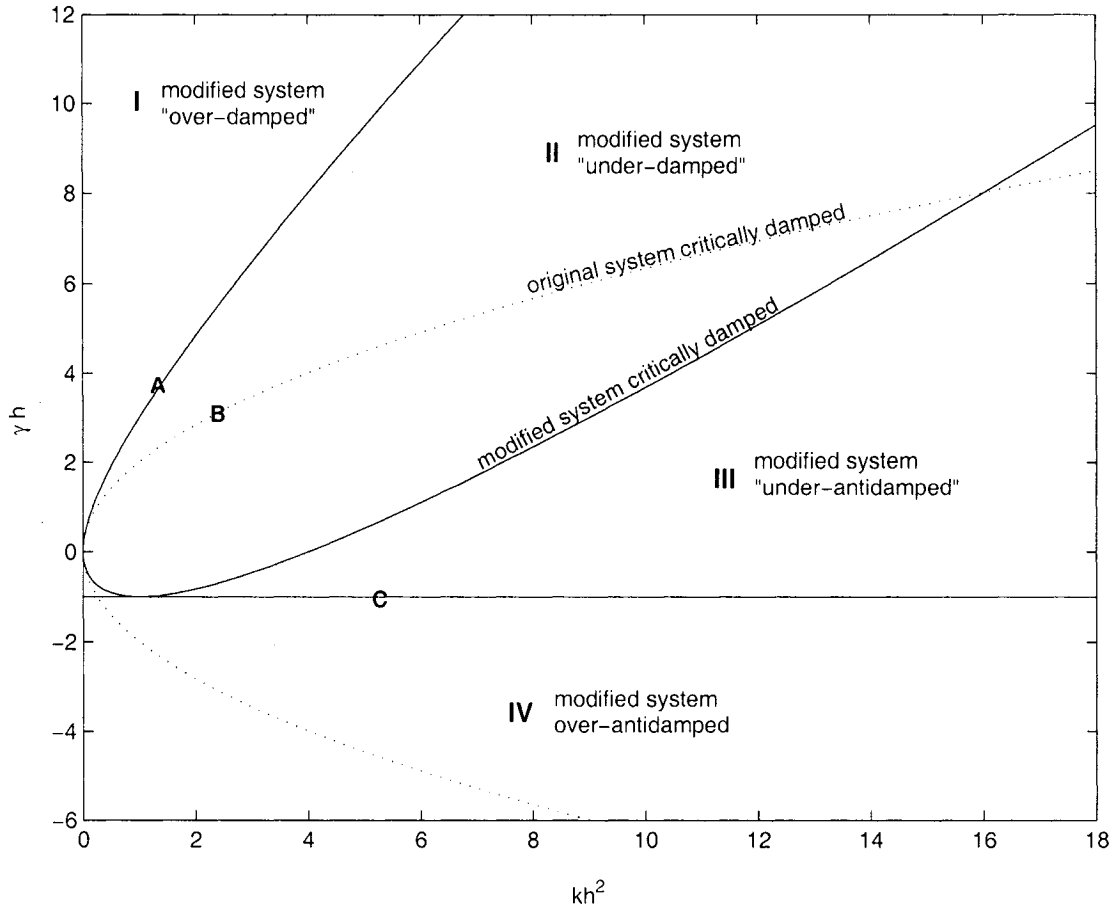


Figure 2.2: The dimensionless parameters kh^2 and γh are very important in characterizing the behaviour of the numerical solutions and the modified system. Though the time step h does not appear in the expression for the eigenvalues of the exact system, we can write an expression in terms of kh^2 and γh by multiplying and dividing by h accordingly (see (2.14)). The lines divide the parameter space into regions where the various modified solutions display under-damped or over-damped behaviour. The dotted line corresponds to the exact system and the solid lines correspond to the modified system and numerical solutions.

that for $\gamma h = -1$ (see curve **C** in Fig. 2.2), an explicit formulation can still be

obtained, though the method in this case is not “consistent” – at least in the sense of the limit $h \rightarrow 0$ keeping $\gamma h = -1$ and k constant:

$$\begin{aligned}(1 - kh^2)x_{n+1} &= x_n \\ (1 - kh^2)v_{n+1} &= khx_n.\end{aligned}$$

For this reason, we will restrict our focus to the case where the method is consistent and the representation (2.11) is obtained.

Looking to (2.7) we have the form of the modified equation and modified operator which we will here write as

$$\dot{\tilde{y}} = \tilde{\mathbf{A}}_h \tilde{y}, \quad \tilde{\mathbf{A}}_h = \frac{1}{h} \ln \left(\frac{1}{1 + \gamma h} (\mathbf{I} + \mathbf{A}_h) \right). \quad (2.12)$$

The \ln series expansion in powers of \mathbf{A}_h is well defined if \mathbf{A}_h is diagonalizable and $\gamma h \neq -1$. If $(\gamma h - kh^2)^2 - 4kh^2 \neq 0$ (see curve **A** in Fig. 2.2), \mathbf{A}_h has two distinct eigenvalues given by

$$\lambda_{h\pm} = \frac{\gamma h - kh^2}{2} \pm \frac{1}{2} \sqrt{(\gamma h - kh^2)^2 - 4kh^2}. \quad (2.13)$$

Thus for all points $(kh^2, \gamma h)$ lying off the curves **A** and **C**, \mathbf{A}_h is diagonalizable, and the \ln series is well defined. Furthermore, if \mathbf{A}_h has eigenvalues $\lambda_{h\pm}$, the eigenvalues of the modified matrix $\tilde{\mathbf{A}}_h$ are given by $\tilde{\lambda}_{h\pm} = \frac{1}{h} \ln(1 + \lambda_{h\pm}) - \frac{1}{h} \ln(1 + \gamma h)$.

We now consider the behaviour of the modified system (and the numerical solutions) in the four regions **I**, **II**, **III** and **IV** of $(kh^2, \gamma h)$ parameter space shown in Fig. 2.2. In the figure, lines divide the parameter space into regions where the various modified solutions display under-damped or over-damped behaviour. The dotted line corresponds to the exact system and the solid lines correspond to the modified system and numerical solutions. Though the time step h does not appear in the exact solution, we can write an expression in terms of kh^2 and γh by multiplying and dividing by h accordingly:

$$\lambda_{\pm}^{exact} = \frac{1}{h} \left(-\frac{\gamma h}{2} \pm \sqrt{(\gamma h)^2 - 4kh^2} \right). \quad (2.14)$$

Setting (2.14) to 0 gives the region of critical damping (curve **B** in Fig. 2.2) and shows the under and over-damped regions of the exact solution.

Region **I**. If $1 + \lambda_{h\pm} \in \mathbb{R}^+$ then $\tilde{\lambda}_{h\pm} \in \mathbb{R}^+$ and the modified system is “over-damped” with positive damping. Since we are exclusively considering the case where the eigenvalues of the exact system (2.9) are complex (under-damped), it makes sense to consider only the cases where the eigenvalues, $\tilde{\lambda}_{h\pm}$, of the modified system (2.12) are also complex. This ensures that where the backward error analysis applies, when we consider collisions with linear restoring force and damping in Chapter 3, the modified solution and the numerical solution will not exhibit completely inelastic behaviour (“sticking”). For this reason, we ignore choices of parameters lying within region **I**.

Region **II**. If we assume $(\gamma h - kh^2)^2 - 4kh^2 < 0$, the eigenvalues $\lambda_{h\pm}$ are complex and hence $\tilde{\lambda}_{h\pm}$ are also complex. Here, the modified system exhibits “under-damped” behaviour with the sign of the effective damping determined by the damping parameter γ . Solutions from region **II** qualitatively capture the dynamics of the exact solution. In this region the eigenvalues of \mathbf{A}_h are given by

$$\lambda_{h\pm} = \frac{\gamma h - kh^2}{2} \pm \frac{1}{2}i\sqrt{4kh^2 - (\gamma h - kh^2)^2} \quad (2.15)$$

with corresponding eigenvectors (two convenient representations are included)

$$\mathbf{v}_{\pm} = \begin{pmatrix} \lambda_{h\pm} \\ -kh \end{pmatrix} \text{ or } \mathbf{v}_{\pm} = \begin{pmatrix} -h \\ \lambda_{h\mp} \end{pmatrix}. \quad (2.16)$$

With $\mathbf{V} = (\mathbf{v}_+ \mathbf{v}_-)$ we have

$$\mathbf{V}^{-1}\mathbf{A}_h\mathbf{V} = \begin{pmatrix} \lambda_{h+} & 0 \\ 0 & \lambda_{h-} \end{pmatrix}$$

and

$$\begin{aligned}
\ln\left(\frac{1}{1+\gamma h}(\mathbf{I} + \mathbf{A}_h)\right) &= \ln(\mathbf{I} - \mathbf{A}_h) - \ln(1 + \gamma h)\mathbf{I} \\
&= \mathbf{V} \ln(\mathbf{I} - \mathbf{V}^{-1}\mathbf{A}_h\mathbf{V})\mathbf{V}^{-1} - \ln(1 + \gamma h)\mathbf{I} \\
&= \mathbf{V} \begin{pmatrix} \ln(1 + \lambda_{h+}) & 0 \\ 0 & \ln(1 + \lambda_{h-}) \end{pmatrix} \mathbf{V}^{-1} - \ln(1 + \gamma h)\mathbf{I}
\end{aligned}$$

Noting that $|1 + \lambda_{h\pm}|^2 = 1 + \gamma h$ and letting $1 + \lambda_{h\pm} = \sqrt{1 + \gamma h}e^{\pm i\theta}$, $\cos \theta = \frac{2 + \gamma h - kh^2}{2\sqrt{1 + \gamma h}}$, we have

$$\ln(1 + \lambda_{h\pm}) = \frac{1}{2} \ln(1 + \gamma h) \pm i\theta$$

Grinding through the matrix multiplication gives

$$\begin{aligned}
\tilde{\mathbf{A}}_h &= \frac{1}{h} \mathbf{V} \begin{pmatrix} \frac{1}{2} \ln(1 + \gamma h) + i\theta & 0 \\ 0 & \frac{1}{2} \ln(1 + \gamma h) - i\theta \end{pmatrix} \mathbf{V}^{-1} - \frac{1}{h} \ln(1 + \gamma h)\mathbf{I} \\
&= -\frac{1}{2h} \ln(1 + \gamma h)\mathbf{I} + \frac{\theta/h}{\sqrt{4kh^2 - (\gamma h - kh^2)^2}} \begin{pmatrix} \gamma h - kh^2 & 2h \\ -2kh & -\gamma h + kh^2 \end{pmatrix} \quad (2.17)
\end{aligned}$$

with $(\gamma h - kh^2)^2 - 4kh^2 < 0$. Checking the limit as $h \rightarrow 0$, holding k and γ constant, we see that

$$\lim_{h \rightarrow 0} \frac{\theta(h)}{\sqrt{4kh^2 - (\gamma h - kh^2)^2}} = \frac{1}{2}, \quad (2.18)$$

$$\lim_{h \rightarrow 0} \frac{\ln(1 + \gamma h)}{h} = \gamma \quad (2.19)$$

and so $\tilde{\mathbf{A}}_h \rightarrow \mathbf{A}$ as $h \rightarrow 0$. Finally, in region **II**, the eigenvalues of the modified linear operator $\tilde{\mathbf{A}}_h$ are given by

$$\tilde{\lambda}_{h\pm} = -\frac{1}{2h} \ln(1 + \gamma h) \pm i\frac{\theta}{h}. \quad (2.20)$$

Furthermore, the modified solution has a period of $\tilde{T} = 2\pi/\text{Im}\tilde{\lambda}_{h\pm} = 2\pi\frac{h}{\theta}$. In Fig. 2.3 the damping effects in modified and numerical solutions from region **II** are at

least qualitatively similar to those of the exact solutions – positive damping leads to decaying amplitudes and negative damping to growing amplitudes.

Region **III**. Assuming $(\gamma h - kh^2)^2 - 4kh^2 > 0$ and $1 + \lambda_{h\pm} < -1$, $\tilde{\lambda}_{h\pm}$ will be given by the logarithm of a negative real number and will therefore be complex. The modified numerical system will again be “under-damped” though the effective damping will be negative. The calculations involved in finding the modified equation are similar to those shown above. It turns out that the modified solutions in region **III** can be obtained simply by taking the real part of the solution from region **II**. Solutions for two choices of parameters $(kh^2, \gamma h)$ lying in region **III** are shown in Fig. 2.4. Unlike in region **II**, positive damping ($\gamma > 0$) does not result in solutions with decaying amplitudes. For any choice of parameters $(kh^2, \gamma h)$ in region **III**, the modified solutions grow exponentially.

Region **IV**. Here the modified solutions are over-damped with negative damping. Solutions diverge to infinity (in both x and v) without oscillations. Since this case falls outside the realm of most applications, the backward error analysis will not be developed here, though the modified equation in region **IV** is well defined.

Knowing the modified equation over the regions of $(kh^2, \gamma h)$ space, modified solutions can be calculated and used to predict the behaviour of the numerical solutions. It is worth noting that the modified equations approach presented here holds for h of any magnitude. The problem of the linear method applied to a linear equation (symplectic Euler with linear-spring) is indeed a special case, as for most problems the exact modified equation exists only as a divergent formal series.

2.2.2 Undamped oscillator with symplectic Euler

We now turn to the undamped simple harmonic oscillator where we apply the backward error analysis to characterize the behaviour of the numerical solution. The spring-mass system with one end fixed (i.e. to a wall of infinite mass) does not con-

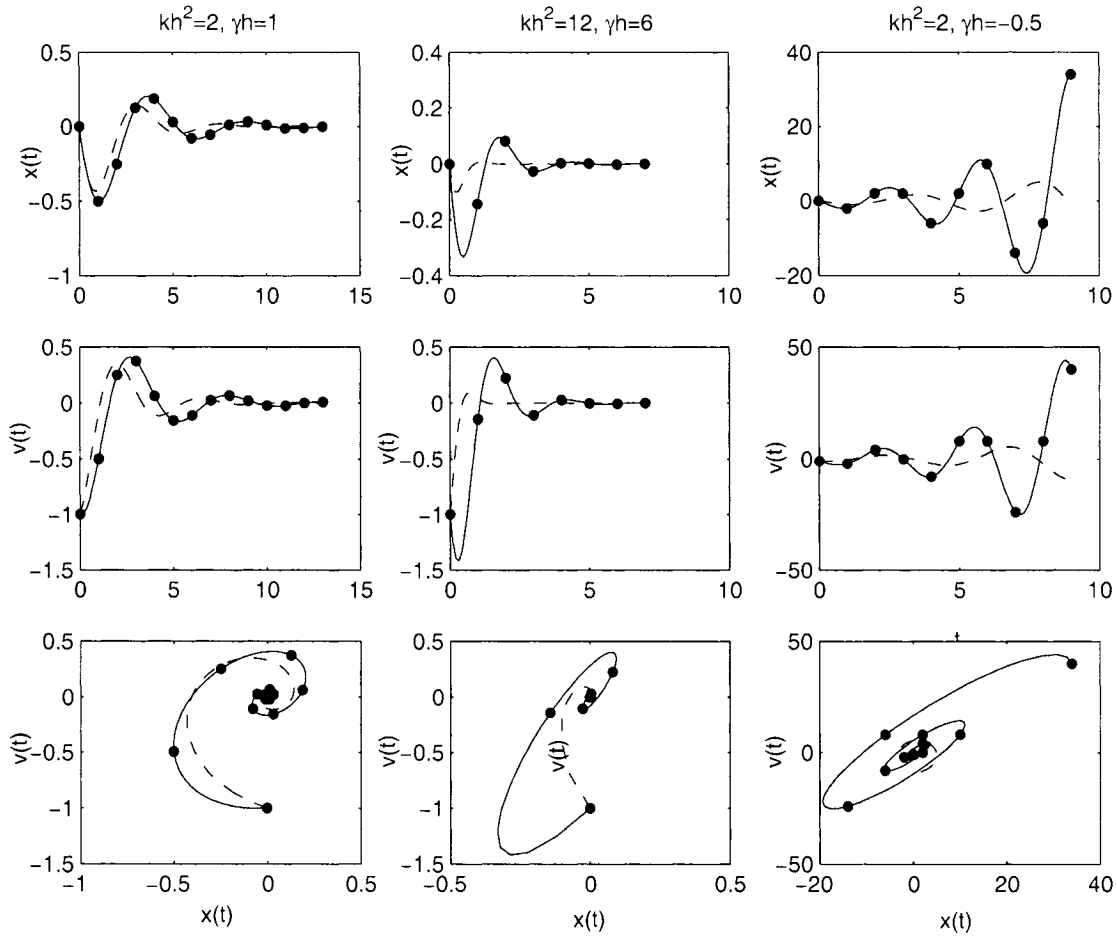


Figure 2.3: Solutions from region **II**. Position and velocity of numerical solutions (points), modified solutions (solid), and exact solutions (dashed) plotted in time and in phase space. In this region, the modified and numerical solutions capture the qualitative dynamics of the exact solution. The sign of the damping in the exact system corresponds to the sign of damping in the modified and numerical system.

serve momentum but does conserve energy. In Chapter 3, we will consider pairwise-interacting particle systems in which both momentum and energy are conserved. Ideally, we would like a numerical method to conserve all first integrals exactly. Since

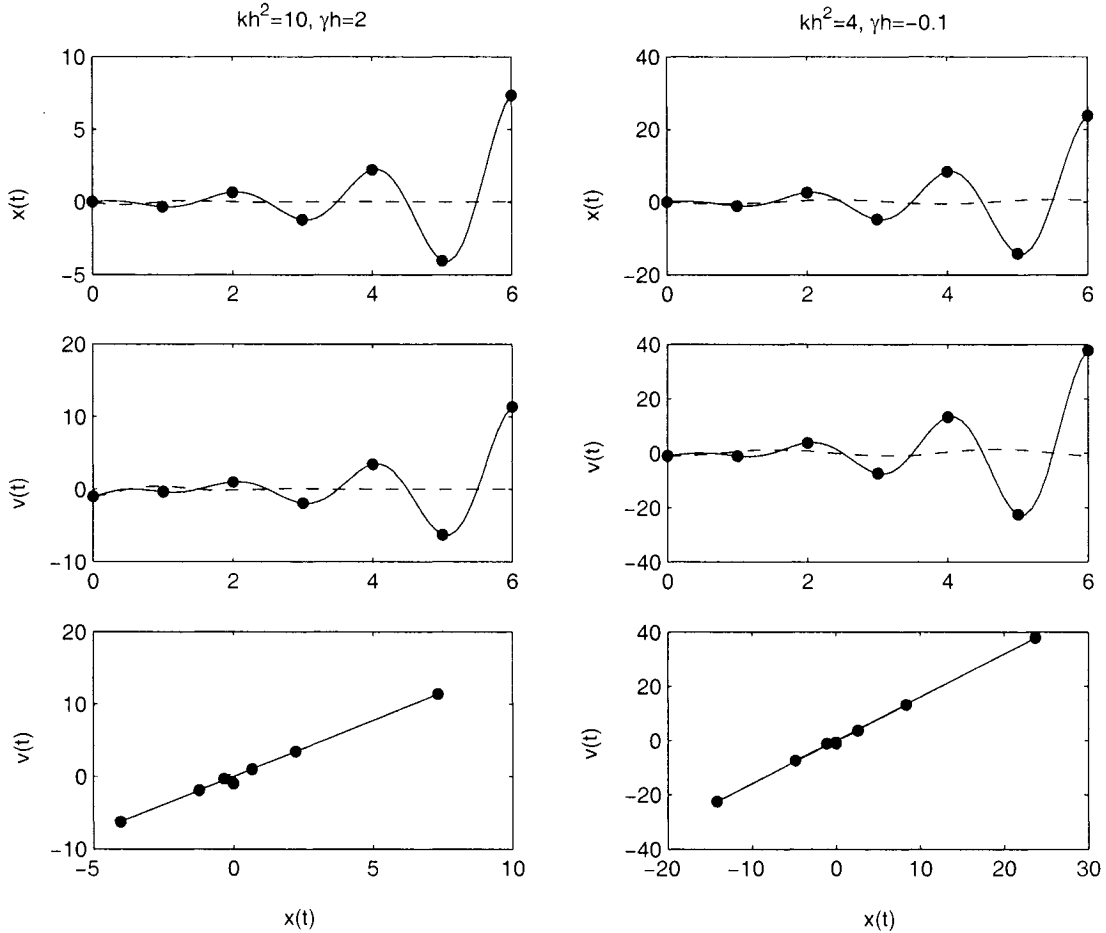


Figure 2.4: Solutions from region **III**. Position and velocity of numerical solutions (points), modified solutions (solid), and exact solutions (dashed) plotted in time and in phase space. Solutions in this region are anti-damped and under-damped regardless of the choice of γ .

momentum, and all linear first integrals in general, are trivially conserved by most methods [25], we will turn our attention to the conservation (or lack thereof) of total energy.

Perhaps more important than the conservation of energy of the undamped system is its Hamiltonian structure. Sanz-Serna [44] notes that while there exist energy

conserving systems which are not Hamiltonian, all Hamiltonian systems are symplectic. Symplecticity is a property which characterizes Hamiltonian systems. Either directly or indirectly, it is probably for this reason that symplectic integrators are often favoured over higher order methods which destroy this structure. In fact the modified equation (or truncated modified equation) of a symplectic method applied to a Hamiltonian system is again Hamiltonian [20], [3]. Furthermore, the modified Hamiltonian and the original Hamiltonian are conserved to a high degree over exponentially long time intervals [3].

For general systems, determining the (truncated) modified Hamiltonian to higher orders often involves lengthy calculations. In the simple linear system presented here, the full modified Hamiltonian is easily obtained from the modified equation given above. Setting $\gamma = 0$ in (2.17), gives

$$\tilde{\mathbf{A}}_h = \frac{\theta/h}{\sqrt{kh^2(4 - kh^2)}} \begin{pmatrix} -kh^2 & 2h \\ -2kh & kh^2 \end{pmatrix} \quad (2.21)$$

where $\cos \theta = \frac{1}{2}(2 - kh^2)$. An equivalent form of the modified Hamiltonian is derived in [8] using the formal series expansion of the modified Hamiltonian. Given the Hamiltonian formulation of the modified undamped system

$$\dot{\tilde{y}} = \mathbf{J}^{-1} \nabla \tilde{\mathcal{H}}_h(\tilde{y}), \quad (2.22)$$

where $\tilde{y} = (\tilde{x}, \tilde{v})^T$ and $\mathbf{J} = \begin{pmatrix} 0 & 1 \\ -1 & 0 \end{pmatrix}$, the modified Hamiltonian, $\tilde{\mathcal{H}}_h$, can be calculated using (2.21) by setting $\dot{\tilde{y}} = \tilde{\mathbf{A}}_h \tilde{y} = \mathbf{J}^{-1} \nabla \tilde{\mathcal{H}}_h(\tilde{y})$. Some simple manipulation yields

$$\tilde{\mathcal{H}}_h(x, v) = \frac{2\theta}{\sqrt{kh^2(4 - kh^2)}} \left(\mathcal{H}(x, v) - \frac{khxv}{2} \right) = \frac{\theta}{\sin \theta} \left(\mathcal{H}(x, v) - \frac{khxv}{2} \right). \quad (2.23)$$

For small h , the proximity of $\tilde{\mathcal{H}}_h$ to \mathcal{H} depends on the parameter kh since from (2.18)

we have that as $kh^2 \rightarrow 0$, $\frac{\theta}{\sin\theta} \approx 1$ and

$$\tilde{\mathcal{H}}_h \approx \mathcal{H} + \mathcal{O}(kh) \tag{2.24}$$

where $\mathcal{H} = \frac{kx^2}{2} + \frac{v^2}{2}$ is the Hamiltonian of the original system. Figures 2.5 and 2.6 show exact, numerical and modified solutions with $\gamma = 0$ for several values of $kh^2 \in (0, 4)$. It should be noted that the symmetry of the points of the numerical solutions in Fig. 2.6 is not coincidental and leads to interesting implications for collisions between particles governed by this same linear restoring force. This will be described and explored further in Chapter 3.

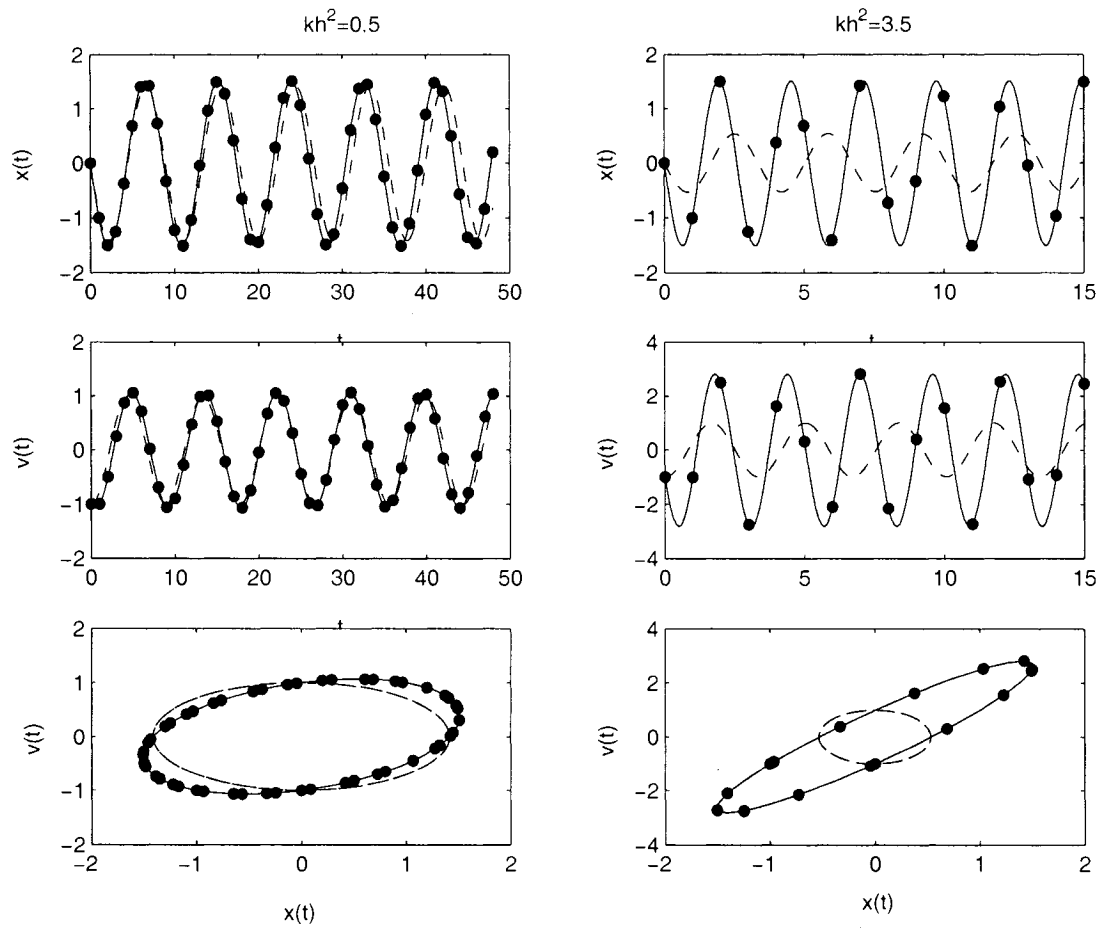


Figure 2.5: Undamped solutions from Region II. Position and velocity of numerical solutions (points), modified solutions (solid), and exact solutions (dashed) plotted in time and in phase space.

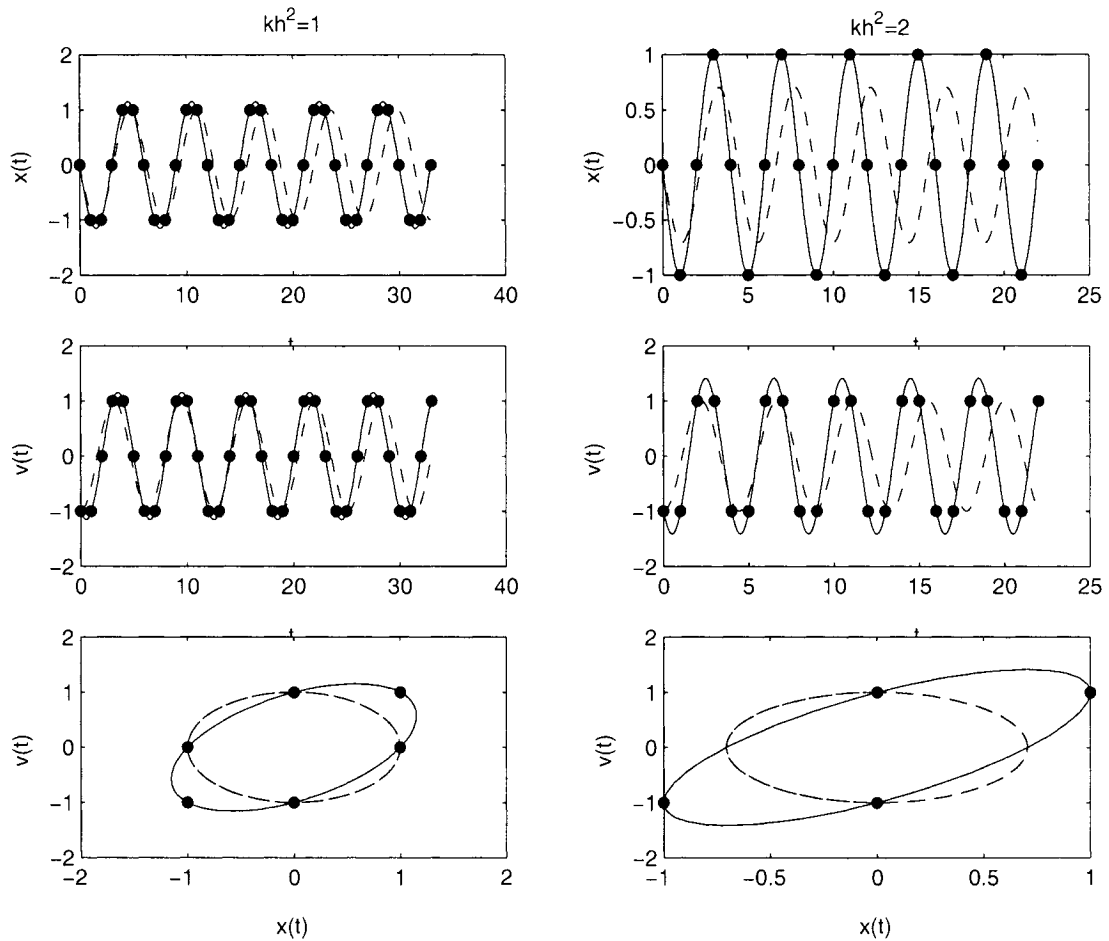


Figure 2.6: Undamped solutions from region II. Position and velocity of numerical solutions (points), modified solutions (solid), and exact solutions (dashed) plotted in time and in phase space. The symmetry of the numerical points is due to the particular choice of the parameter kh^2 (or equivalently θ).

Chapter 3

Numerical Approximation of a Simple Collision

In molecular dynamics simulations, one often considers models in which particles interact (solely) by a pairwise potential. If this potential is non-local, an artificial cut-off can be introduced in implementations to avoid finite box-size effects such as particle self-interaction in periodic domains. For cut-offs based on interparticle distances which are sufficiently small, and for sufficiently low particle densities, we may speak of inter-particle interactions in terms of collisions and say that multiple particle collisions are rare.

Effects of interaction force cut-offs, that is cut-offs based on the magnitude of the interaction force rather than the interparticle distance, are considered by Skeel [49] and analyzed in the context of rounding error and numerical (in)stability. The situation of higher densities or larger distance cut-offs where multiple-particle interactions (collisions) are significant might be at least partially explained by a similar treatment.

In this chapter we investigate a collision between a particle and a wall governed by the linear restoring and damping forces (2.9) given in Chapter 2. In Chapter 4, the two-particle collision is shown to be equivalent to the particle-wall collision un-

der an appropriate change of variables. The strictly local interaction of the particle and wall involves a cut-off of the potential when the distance of separation between the particle and the wall is positive. Applying the symplectic Euler method to this collision problem yields error in the post-collision velocity of the particle. This error can be viewed as a combination of error introduced by the method while integrating the collision forces and error due to the cut-off. Here, the post-collision energy is predicted using backward error analysis and is shown to be in agreement with numerical computations.

3.1 Error due to particle-wall collisions

We now consider simple collisions in one dimension involving a single particle and a wall governed by a linear restoring force and use the results of Chapter 2 to analyze the error in energy introduced by the symplectic Euler method (1.5) and by the discretization of time. The analysis for the particle-wall collision presented here can be extended in a similar manner for the relative velocity of colliding particles in one dimension. In Chapter 4, a simple extension of the analysis allows a full description of the two-particle collision.

For dynamical systems of the form (2.1) where f is analytic and the formal series (2.5) converges, the modified equation approach presented in Chapter 2 can be applied to exactly determine (up to machine precision) the error induced by the numerical approximation. In many cases f is not analytic or, as in most cases, the formal series (2.5) is divergent. In these former cases the modified equation can only be defined up to some finite power in h . If f is piecewise analytic, however, we can calculate solutions of the truncated modified equation in each of the regions where f is smooth and attempt to match the solutions at the edges, obtaining a piecewise modified solution. In the situation presented here, the system is piecewise linear and

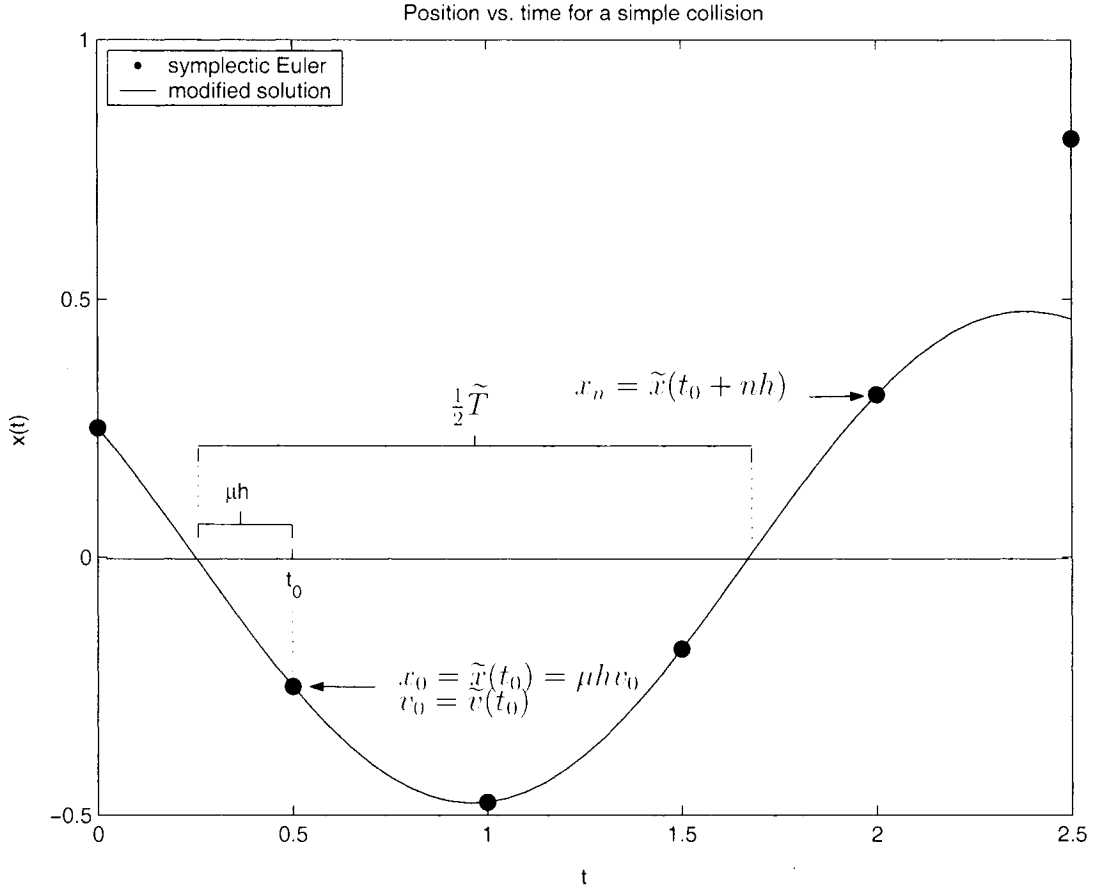


Figure 3.1: Position versus time for a simple collision between a particle and a wall of infinite mass. The numerical solution is plotted as points and the modified solution, \tilde{x} , from the region \mathcal{R}_{coll} is the solid line. Note that \tilde{x} is extended into the region \mathcal{R}_{free} for illustrative purposes – \tilde{x} is the solution of the modified equation in \mathcal{R}_{coll} with initial conditions given by the numerical solution at time t_0 .

a piecewise linear exact (not truncated) modified equation can be obtained.

For particle-wall collisions where particles are either in free motion or are subject to a local interaction with a flat wall, the dynamics can be reduced to one-dimension

normal to the wall. The system is then given by

$$\begin{pmatrix} \dot{x} \\ \dot{v} \end{pmatrix} = \begin{cases} f(x, v), & x < 0 \\ 0, & x \geq 0 \end{cases} \quad (3.1)$$

where $x + \frac{d}{2}$ is the distance between the centre the particle of diameter d and the wall and v is the velocity of the particle in the direction perpendicular to the wall. Consider (3.1) with initial conditions $x(0) = x_0, v(0) = v_0$ and the method Φ_h with numerical solution $\{y_n\}_{n=0}^\infty$. Let

$$\mathcal{R}_{free} = \{(x, v) | x \geq 0\}. \quad (3.2)$$

$$\mathcal{R}_{coll} = \{(x, v) | x < 0\} \quad (3.3)$$

and let \tilde{y} be the modified solution from Chapter 2 with initial conditions

$$\tilde{y}(t_0) = (\mu(x_0, v_0)h v_0, v_0)^T \quad (3.4)$$

where h is the step size and $\mu(x_0, v_0) \in [0, 1)$ is a function of the initial conditions as explained below. Fig. 3.1 illustrates this set up. For the case of the free particle in \mathcal{R}_{free} , the right hand side of (3.1) is 0 and hence the modified equation in this region will be equal to the exact solution for any reasonable method. Since the numerical solution is defined only at discrete points in time, we can not give initial conditions at the boundary of \mathcal{R}_{free} and \mathcal{R}_{coll} , but must define the conditions at the first point in the time discretization where the numerical solution enters \mathcal{R}_{coll} . In effect, the numerically integrated solution “feels” the interaction force slightly too late, when the particles are already overlapping. This overlap is completely determined by the initial conditions and the time step h . Since in \mathcal{R}_{free} the numerical solution is the exact constant velocity solution, this overlap is non-negative and can be no greater than $v_0 h$ and in general will be given by $\mu(x_0, v_0)v_0 h$. Notice that when the duration of the collision is several times the step size, h , the modified equation is a physically reasonable interpolant of the points at $t_0 - h$ and t_0 .

The primary interest in this investigation is the statistical behaviour of the energy of the numerically integrated system. Using the piecewise-matched solutions of the modified equation for the particle-wall collision we can determine the post-collision energy as a function of the parameters kh^2 , μ and v_0 . To calculate the energy change of the numerical solution due to a collision we seek the value of v_n at the first point of re-entry into region \mathcal{R}_{free} (immediately after the collision). That is we are interested in $\tilde{v}(t_0+nh)$ where n is the number of time steps between the first point in and the first point out of \mathcal{R}_{coll} . Finding an expression for n amounts to finding the length of the interval between two successive roots of $\tilde{x}(t)$. Once an expression for the post-collision energy is obtained, if the variable μ is assumed to be an appropriately distributed random variable, various statistics of the numerical solution can be calculated. The details of the calculations for the damped and undamped linear spring collision are presented below.

3.1.1 Damped linear-spring collision with the symplectic Euler method

Here we consider the case of the damped linear-spring collision with the symplectic Euler method and apply the results of Subsection 2.2.1 to the collision problem as described above. To compute the modified solution we need only solve (2.12) with the appropriate initial conditions. We solve

$$\tilde{y} = \tilde{\mathbf{A}}_h \tilde{y}, \quad \tilde{y}(0) = (\mu h v_0, v_0)^T \quad (3.5)$$

where

$$\tilde{\mathbf{A}}_h = \frac{1}{h} \ln \left(\frac{1}{1 + \gamma h} (\mathbf{I} + \mathbf{A}_h) \right), \quad \mathbf{A}_h = \begin{pmatrix} \gamma h - kh^2 & h \\ -kh & 0 \end{pmatrix}$$

The solution is given by

$$\tilde{y}(t) = e^{t\tilde{\mathbf{A}}_h} \begin{pmatrix} \mu h v_0 \\ v_0 \end{pmatrix}. \quad (3.6)$$

It happens that $\tilde{\mathbf{A}}_h$ is just a linear combination of powers of \mathbf{A}_h and hence has the same eigenvectors with corresponding eigenvalues $\tilde{\lambda}_{h\pm}$ (2.20). Reusing the matrix V defined in Subsection 2.2.1, we have

$$\begin{aligned} \tilde{y}(t) &= \mathbf{V} \begin{pmatrix} e^{\tilde{\lambda}_+ t} & 0 \\ 0 & e^{\tilde{\lambda}_- t} \end{pmatrix} \mathbf{V}^{-1} \begin{pmatrix} \mu h v_0 \\ v_0 \end{pmatrix} \\ &= \mathbf{V} \begin{pmatrix} e^{(-\frac{1}{2h} \ln(1+\gamma h) + i\frac{\theta}{h})t} & 0 \\ 0 & e^{(-\frac{1}{2h} \ln(1+\gamma h) - i\frac{\theta}{h})t} \end{pmatrix} \mathbf{V}^{-1} \begin{pmatrix} \mu h v_0 \\ v_0 \end{pmatrix} \\ &= \left(\frac{1}{1+\gamma h} \right)^{\frac{t}{2h}} \mathbf{V} \begin{pmatrix} e^{i\frac{\theta}{h}t} & 0 \\ 0 & e^{-i\frac{\theta}{h}t} \end{pmatrix} \mathbf{V}^{-1} \begin{pmatrix} \mu h v_0 \\ v_0 \end{pmatrix} \\ &= \begin{pmatrix} \cos(\frac{\theta}{h}t) - \frac{-\gamma h + kh^2}{\sqrt{4kh^2 - (\gamma h - kh^2)^2}} \sin(\frac{\theta}{h}t) & \frac{2h}{\sqrt{4kh^2 - (\gamma h - kh^2)^2}} \sin(\frac{\theta}{h}t) \\ -\frac{2kh}{\sqrt{4kh^2 - (\gamma h - kh^2)^2}} \sin(\frac{\theta}{h}t) & \cos(\frac{\theta}{h}t) + \frac{-\gamma h + kh^2}{\sqrt{4kh^2 - (\gamma h - kh^2)^2}} \sin(\frac{\theta}{h}t) \end{pmatrix} \\ &\quad \cdot \begin{pmatrix} \mu h v_0 \\ v_0 \end{pmatrix} \left(\frac{1}{1+\gamma h} \right)^{\frac{t}{2h}} \end{aligned} \quad (3.7)$$

where $\cos \theta = \frac{2+\gamma h - kh^2}{2\sqrt{1+\gamma h}}$ (see Subsection 2.2.1). Multiplying through and simplifying, we obtain expressions of $\tilde{v}(t)$ and $\tilde{x}(t)$:

$$\tilde{v}(t) = (1+\gamma h)^{-\frac{t}{2h}} \left(\cos\left(\frac{t}{h}\theta\right) - \frac{\gamma h - kh^2(1-2\mu)}{\sqrt{4\gamma h - (\gamma h - kh^2)^2}} \sin\left(\frac{t}{h}\theta\right) \right) v_0 \quad (3.8)$$

$$\tilde{x}(t) = (1+\gamma h)^{-\frac{t}{2h}} \left(\mu \cos\left(\frac{t}{h}\theta\right) + \frac{2 + (\gamma h - kh^2)\mu}{\sqrt{4\gamma h - (\gamma h - kh^2)^2}} \sin\left(\frac{t}{h}\theta\right) \right) h v_0. \quad (3.9)$$

To find the energy of the particle after the collision we look for the value of the modified velocity, \tilde{v} , at the time $t_n = t_0 + nh$ where t_n is the time at which the numerical solution re-enters region \mathcal{R}_{free} . This means that n is the unique integer

such that $x_0 \leq 0, x_1 \leq 0, \dots, x_{n-2} \leq 0, x_{n-1} < 0$ and $x_n \geq 0$ (i.e. n is the number of points in the collision). Let $t_0 = 0$ and $\mu' \in [0, 1)$ such that $\tilde{x}(-\mu'h) = 0$ as in Fig. 3.2. Then since the modified solution in \mathcal{R}_{coll} oscillates with period \tilde{T} , the time between collision entry and exit (total time in \mathcal{R}_{coll}) is half this period, $\frac{\tilde{T}}{2}$ (see Fig. 3.2). Since μ' solves $\tilde{x}(-\mu'h) = 0$, and $\tilde{x}(t)$ depends on kh^2, γ and μ , we will in general have the dependence $\mu' = \mu'(kh^2, \gamma h, \mu)$. We also see that $\theta = \theta(kh^2, \gamma h)$ and the integer $n = n(kh^2, \gamma h, \mu)$ is given by

$$n = \left\lceil \frac{\tilde{T}/2 - \mu'h}{h} \right\rceil = \left\lceil \frac{\pi}{\theta} - \mu' \right\rceil. \quad (3.10)$$

Combining (3.10) and (3.8) we obtain an expression for the relative change in energy:

$$\frac{E_f}{E_0}(\mu, kh^2, \gamma h) = \left(\frac{\tilde{v}(nh)}{v_0} \right)^2 \quad (3.11)$$

$$= (1 + \gamma h)^{-\frac{n}{2}} \left(\cos(n\theta) - \frac{\gamma h - kh^2(1 - 2\mu)}{\sqrt{4kh^2 - (\gamma h - kh^2)^2}} \sin(n\theta) \right)^2. \quad (3.12)$$

It should be noted that n and θ are functions of the parameters $kh^2, \gamma h$ and μ but are written without arguments for ease of notation. Fig. 3.3 shows the relative change in energy, $\frac{E_f}{E_0}$, as a function of μ for $kh^2 = 2$ and several values of γh . Results from both numerical experiments (points) and backward error analysis (solid) are plotted to show that rounding error is not significant. For $\gamma \neq 0$, there is a discontinuous jump in $\frac{E_f}{E_0}$ as μ varies, while when $\gamma = 0$ as in Fig. 3.5 and 3.6, the dependence is continuous. For certain values of θ , the energy change is constant with respect to μ . This is illustrated by Fig. 3.4 and by the horizontal lines in Fig. 3.5 and 3.6. In the undamped system, these lines correspond to perfect energy conservation and are described in detail in Proposition 3.1.

3.1.2 Undamped linear-spring collision with the symplectic Euler method

For the undamped collision, the change in energy is given by (3.11) with $\gamma = 0$:

$$\frac{E_f}{E_0}(\mu, kh^2) = \left(\cos(n\theta) + \frac{kh^2(1-2\mu)}{\sqrt{kh^2(4-kh^2)}} \sin(n\theta) \right)^2. \quad (3.13)$$

This expression can be simplified by noticing that in the undamped case, $\cos(\theta) = (2 - kh^2)/2 \Rightarrow kh^2 = 2 - 2\cos(\theta)$, and replacing kh^2 in (3.11) accordingly. This gives

$$\frac{E_f}{E_0}(\mu, \theta) = \left(\cos(n\theta) + \frac{(1 - \cos \theta)(1 - 2\mu)}{\sin \theta} \sin(n\theta) \right)^2 \quad (3.14)$$

where $\theta \in [0, \pi)$ and n is now a function of μ and θ .

A remarkable implication follows from this expression: for certain choices of θ (or equivalently, certain choices of kh^2), the quantity $E_f/E_0 = 1$ for all $\mu \in [0, 1)$. That is, for these choices of parameters, the numerical integration exactly conserves energy across the collision.

Proposition 3.1. *Let $m \geq 2$, $m \in \mathbb{N}$ and choose kh^2 such that $\theta = \cos^{-1}(\frac{2-kh^2}{2}) = \frac{\pi}{m}$. Then $n(\mu, \theta) = m$, $\forall \mu \in [0, 1)$ and, for collisions between a particle and a wall interacting via a linear-spring potential in one dimension, the symplectic Euler method conserves energy exactly.*

Before proving Proposition 3.1 we need to consider (3.7) in the undamped case and solve $\tilde{x}(-\mu'h) = 0$ obtaining an expression for μ' . Leaving out the details we see that

$$\begin{aligned} \mu'(\mu, kh^2) &= \frac{1}{\theta} \tan^{-1} \left(\frac{\mu \sqrt{kh^2(4-kh^2)}}{2 - \mu kh^2} \right) \\ \Rightarrow \mu'(\mu, \theta) &= \frac{1}{\theta} \tan^{-1} \left(\frac{\mu \sin \theta}{1 - \mu(1 - \cos \theta)} \right). \end{aligned} \quad (3.15)$$

Proof. (Proposition 3.1) Suppose $\theta = \frac{\pi}{m}$ for some $m \geq 2$. For $\theta \leq \frac{\pi}{2}$, μ' is a strictly increasing function of $\mu \in [0, 1)$ since \tan^{-1} is increasing over all of \mathbb{R} . Thus

$$\mu'(\mu, \theta) < \mu'(1, \theta) = \frac{m}{\pi} \tan^{-1} \left(\frac{\sin \frac{\pi}{m}}{\cos \frac{\pi}{m}} \right) = \frac{m}{\pi} \tan^{-1} \tan \frac{\pi}{m} = 1. \quad (3.16)$$

So with $\theta = \frac{\pi}{m}$, $\mu' < 1$ and we have that

$$n(\mu, \theta) = \left\lceil \frac{\pi}{\theta} - \mu' \right\rceil = \lceil m - \mu' \rceil = m. \quad (3.17)$$

Since n is a constant with respect to μ we can plug $\theta = \frac{\pi}{m}$, $n(\mu, \theta) = m$ into (3.14) to verify the proposition:

$$\frac{E_f}{E_0}(\mu, \theta) = \left(\cos(m \frac{\pi}{m}) + \frac{(1 - \cos \frac{\pi}{m})(1 - 2\mu)}{\sin \frac{\pi}{m}} \sin(m \frac{\pi}{m}) \right)^2 = 1. \quad (3.18)$$

Therefore the energy is conserved exactly. \square

In general, the symplectic Euler method does not conserve energy across the collisions. To estimate the effect of these non-conservative collisions in a system of many particles, μ is assumed to be a uniformly distributed random variable and statistics taken over the initial conditions of collisions are calculated. For example, the μ -averaged energy change over undamped collisions is given by

$$\left\langle \frac{E_f}{E_0} \right\rangle_{\mu} = \frac{1}{6} \frac{(\sin(m+1)\theta - \sin m\theta)^6 - \sin^6 \theta}{(\cos \theta - 1) \sin m\theta \sin(m+1)\theta \sin^2 \theta (\sin(m+1)\theta - \sin m\theta)^2} \quad (3.19)$$

where m is the unique integer satisfying

$$\frac{\pi}{m+1} \leq \frac{\pi}{n(\mu, \theta)} \leq \frac{\pi}{m}, \quad \forall \mu \in [0, 1) \quad (3.20)$$

(m is simply the minimum number of time steps in the collision over the range of initial conditions). The quantity $\langle \frac{E_f}{E_0} \rangle_{\mu}$ is never less than one. The μ -averaged energy change with $\gamma = 0$ is shown in Fig. 3.7. The regions **II** and **III** correspond to those in Fig. 2.2. In Fig. 3.8, the change is plotted as a function of θ over part of region **II** where $0 \leq \theta \leq \frac{\pi}{2}$ ($0 \leq kh^2 \leq 2$). Averages for the general undamped collisions

are shown in Fig. 3.10. The “troughs” correspond to $\theta = \frac{\pi}{n}, n = 2, 3, \dots$ as in the undamped case. Lines of constant θ are shown in Fig. 3.9 for comparison.

For simulations, it will be useful to know the maximum penetration depth or overlap during a collision given the parameters θ and v_0 . It is important to choose these parameters so that the maximum overlap of particles does not exceed their diameter. This ensures that the centres of the particles do not cross and the particles do not pass through each other during head-on collisions. Since the modified solution, \tilde{x} , is zero at $t = -\mu' h$ and oscillates with a period of $\tilde{T} = 2\pi h/\theta$, we expect \tilde{x} to attain a maximum amplitude at $t = \tilde{T}/4 - \mu' h$. Looking to (3.9) we set $\gamma = 0$ and plug in $t = \tilde{T}/4 - \mu' h$.

$$\begin{aligned}\tilde{x}\left(\frac{\tilde{T}}{4} - \mu' h\right) &= \left(\mu \cos\left(\frac{\pi}{2} - \mu'\theta\right) + \frac{1 - \mu(1 - \cos\theta)}{\sin\theta} \sin\left(\frac{\pi}{2} - \mu'\theta\right)\right) h v_0 \\ &= \left(-\mu \sin(\mu'\theta) + \frac{1 - \mu(1 - \cos\theta)}{\sin\theta} \cos(\mu'\theta)\right) h v_0 \\ &= \left(-\mu \sin\left(\tan^{-1}\left(\frac{\mu \sin\theta}{1 - \mu(1 - \cos\theta)}\right)\right)\right) \\ &\quad + \frac{1 - \mu(1 - \cos\theta)}{\sin\theta} \cos\left(\tan^{-1}\left(\frac{\mu \sin\theta}{1 - \mu(1 - \cos\theta)}\right)\right) h v_0\end{aligned}$$

Letting $a = \frac{\mu \sin\theta}{1 - \mu(1 - \cos\theta)}$ and using the identities $\cos(\tan^{-1} a) = 1/\sqrt{1 + a^2}$ and $\sin(\tan^{-1} a) = a/\sqrt{1 + a^2}$ we have

$$\begin{aligned}\dots &= \left(-\sin(\tan^{-1} a) + \frac{1}{a} \cos(\tan^{-1} a)\right) \mu h v_0 \\ &= \left(-\frac{a}{\sqrt{1 + a^2}} + \frac{1}{a\sqrt{1 + a^2}}\right) \mu h v_0 = \left(\frac{1 - a^2}{a\sqrt{1 + a^2}}\right) \mu h v_0\end{aligned}$$

It can be shown that for a given θ , this quantity is maximized when $\mu \rightarrow 0$. Taking this limit yields

$$\lim_{\mu \rightarrow 0} \left(\frac{1 - a^2}{a\sqrt{1 + a^2}}\right) \mu h v_0 = \frac{h v_0}{\sin\theta}. \quad (3.21)$$

If twice the particle radius $2r > \frac{v_0 h}{\sin \theta}$, it is guaranteed that the centres of the particles (in one dimension) will not cross.

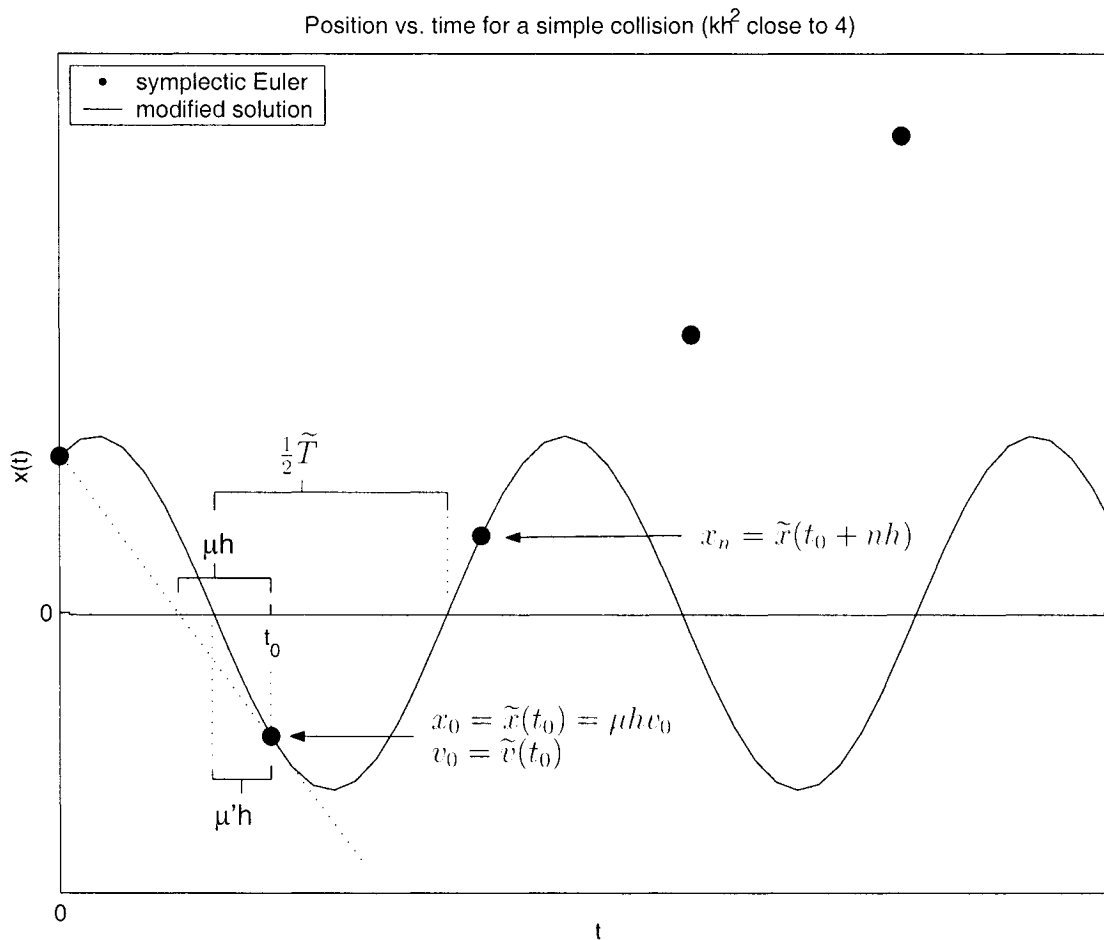


Figure 3.2: Position versus time for a simple particle-wall collision in one dimension. Again, the numerical solution is plotted as points and the modified solution \tilde{x} is extended and plotted as a solid line. Here the collision is stiffer than in Fig. 3.1 in the sense that the dimensionless parameter kh^2 is larger. When the collision is stiffer, only one or two points sample the collision and the modified equation offers an interpolation to the numerical solution which is not as physically reasonable. The time $t_0 - \mu'h$ is when \tilde{x} , extended backwards in time, crosses the x -axis. The time $t_0 - \mu h$ is when the interpolated linear trajectory of the particle crosses the x -axis. As kh^2 increases, the modified period decreases, and the difference $|\mu - \mu'|$ grows.

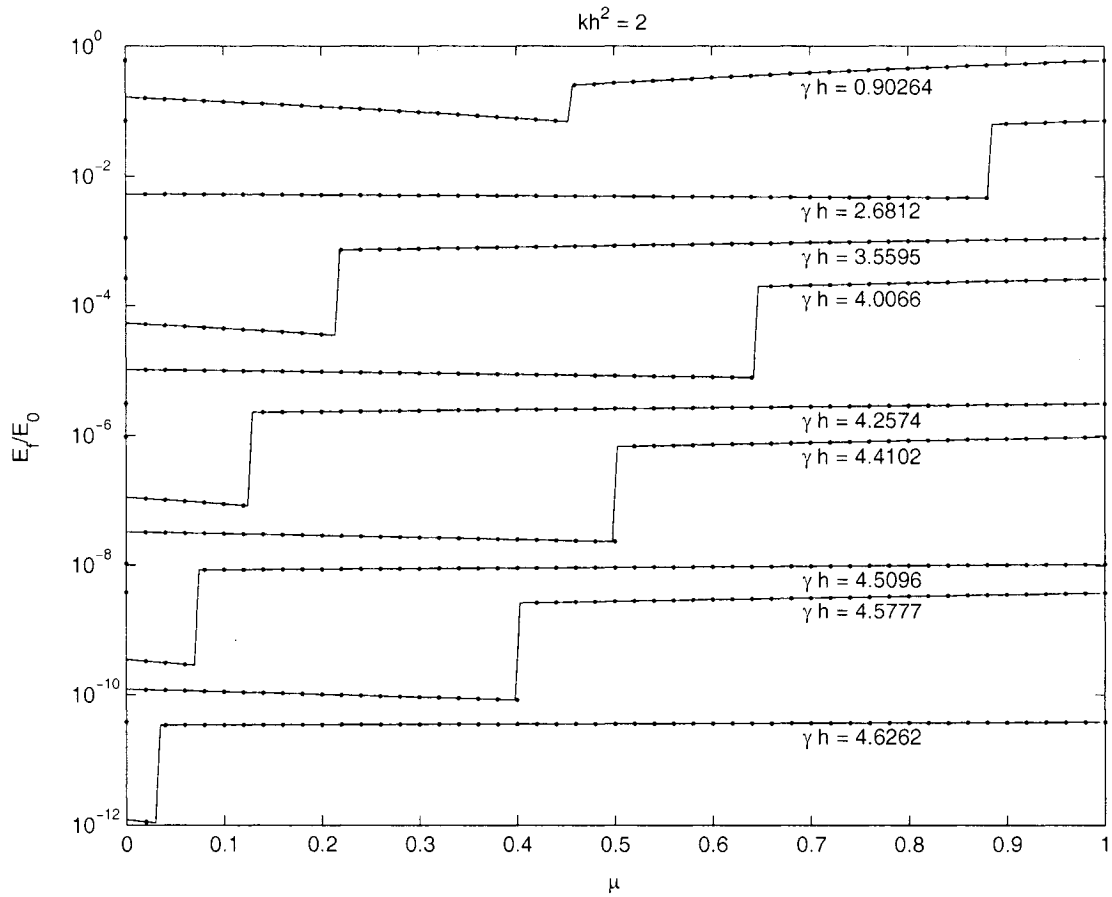


Figure 3.3: Relative change in energy from numerical experiments (points) and the backward error analysis (solid) plotted as a function of μ for $kh^2 = 2$ and several values of γh .

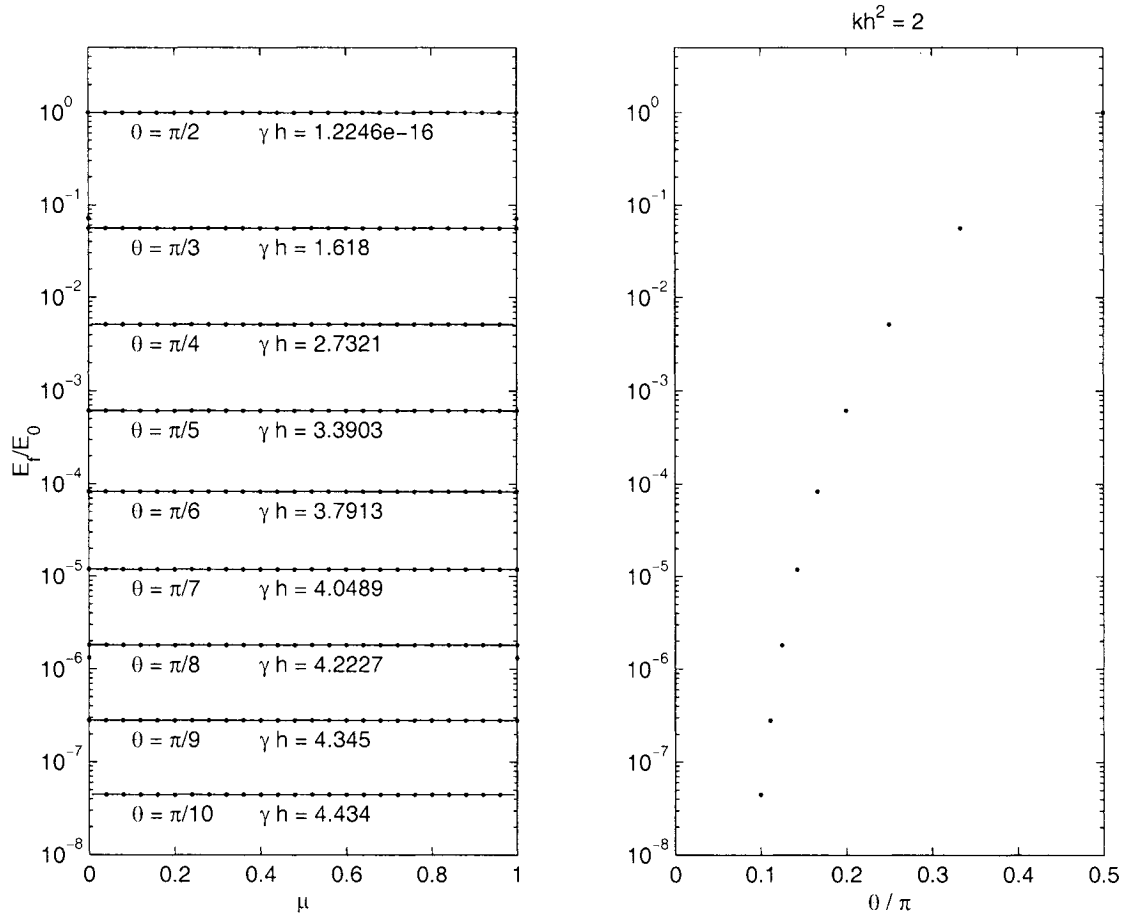


Figure 3.4: Left: Relative change in energy plotted as a function of μ for $\theta = \frac{\pi}{n}$, $n = 2, 3, \dots, 10$. Theoretical change from backward error analysis (solid) and numerical experiments (points) are shown for comparison. Right: Relative change in energy plotted as a function of θ . For any $\theta = \frac{\pi}{n}$, $n \geq 2$, the energy changes by a constant factor dependent on θ for all initial conditions (all μ) and if $\gamma = 0$, the energy is exactly conserved. In this plot the parameters k and h are held constant and θ is varied by changing γ .

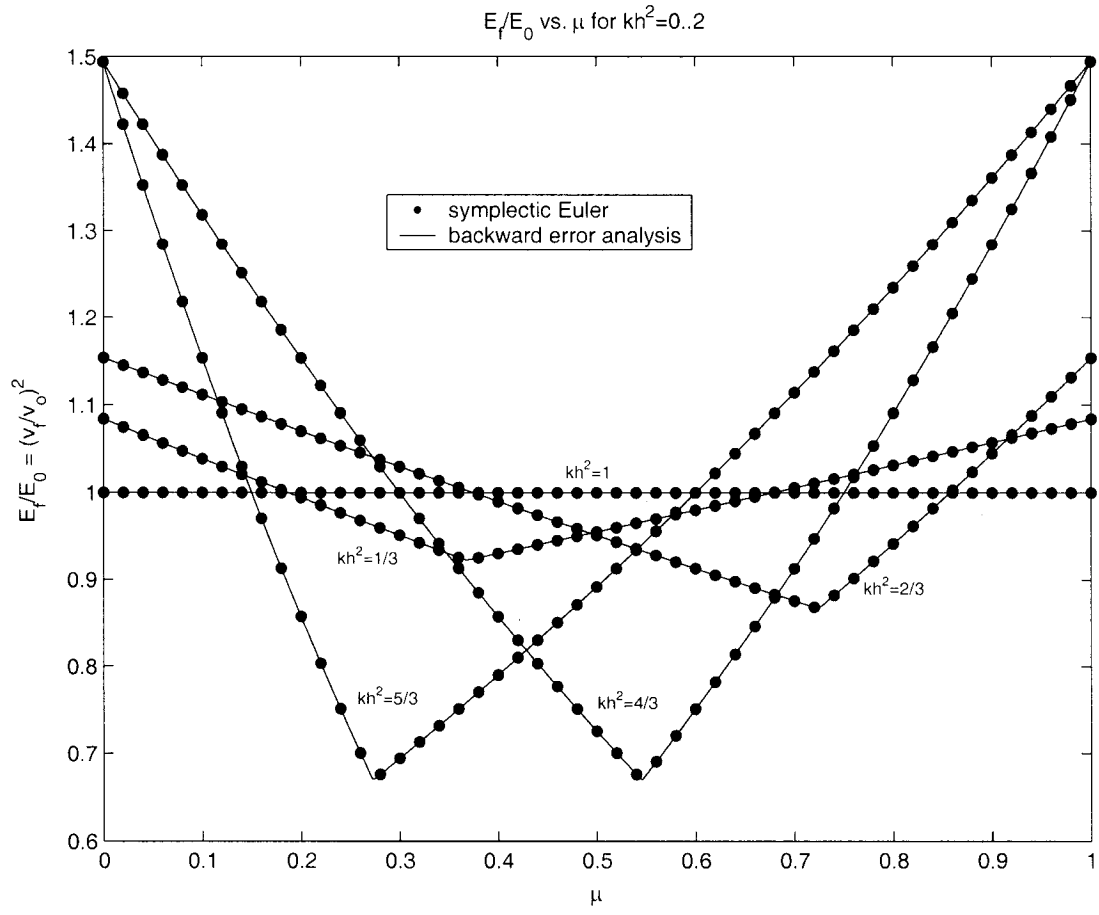


Figure 3.5: Relative change in energy plotted as a function of μ for several values of kh^2 and $\gamma = 0$. The horizontal line corresponds to $\theta = \frac{\pi}{3}$ ($kh^2 = 1$).

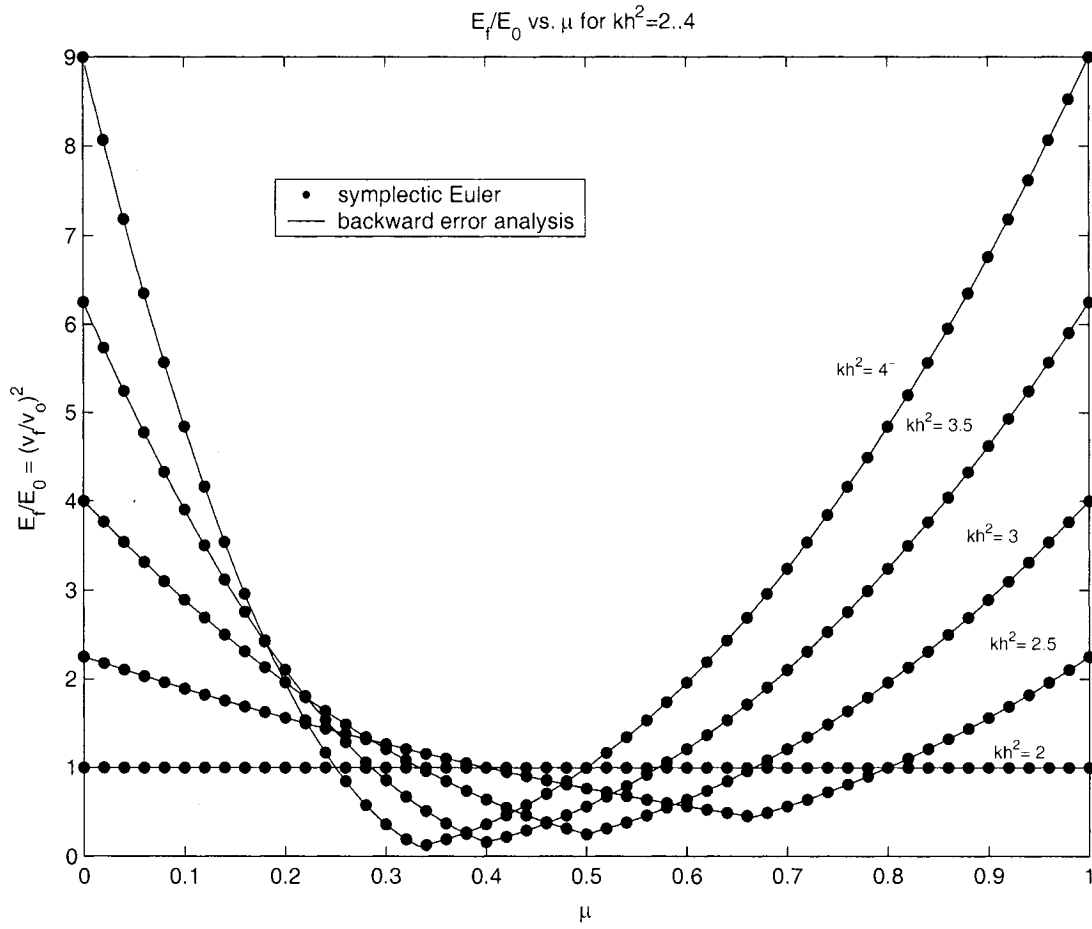


Figure 3.6: Relative change in energy plotted as a function of μ for several values of kh^2 and $\gamma = 0$. The horizontal line corresponds to $\theta = \frac{\pi}{2}$ ($kh^2 = 2$).

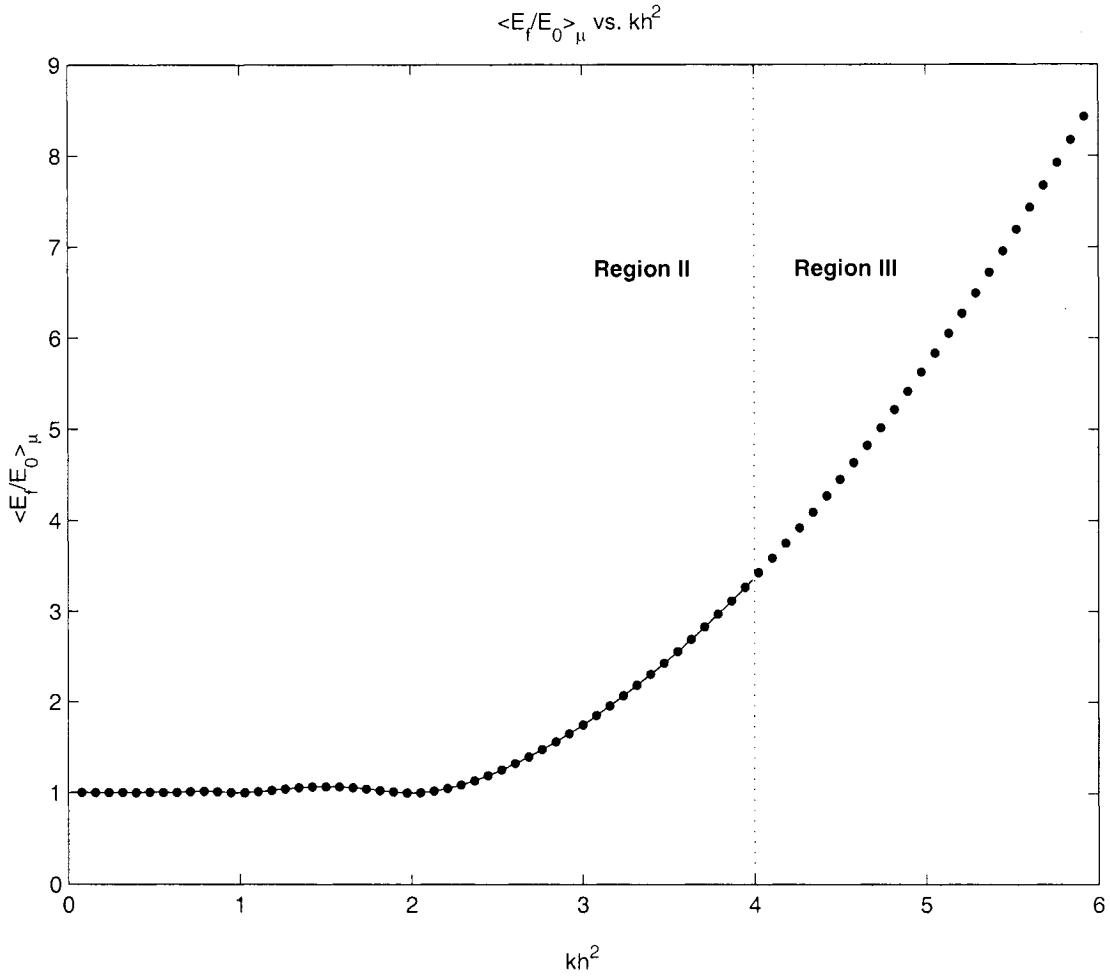


Figure 3.7: μ -averaged change in energy versus kh^2 for undamped linear-spring collisions. Points represent numerical experiments and the solid line the theoretical change from backward error analysis. There is no change in energy for $kh^2 = 2 - 2 \cos(\pi/n)$ for $n = 2, 3, \dots$, but for all other values the energy increases on average. The backward error analysis is restricted to region **II** solely for reasons of convenience.

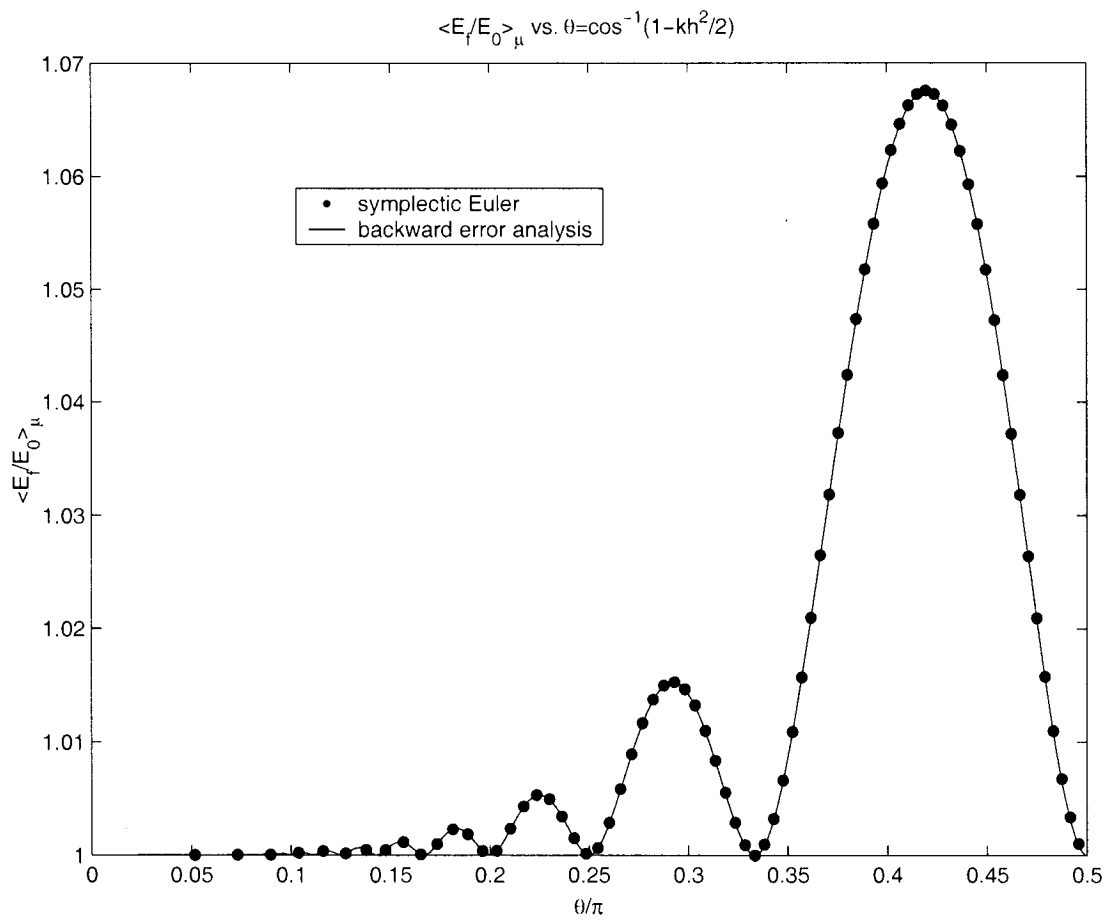


Figure 3.8: Relative change in energy versus θ . The range corresponds to $0 \leq kh^2 \leq 2$, which is the same as that of the curve lying in region **II** of Fig. 3.7.

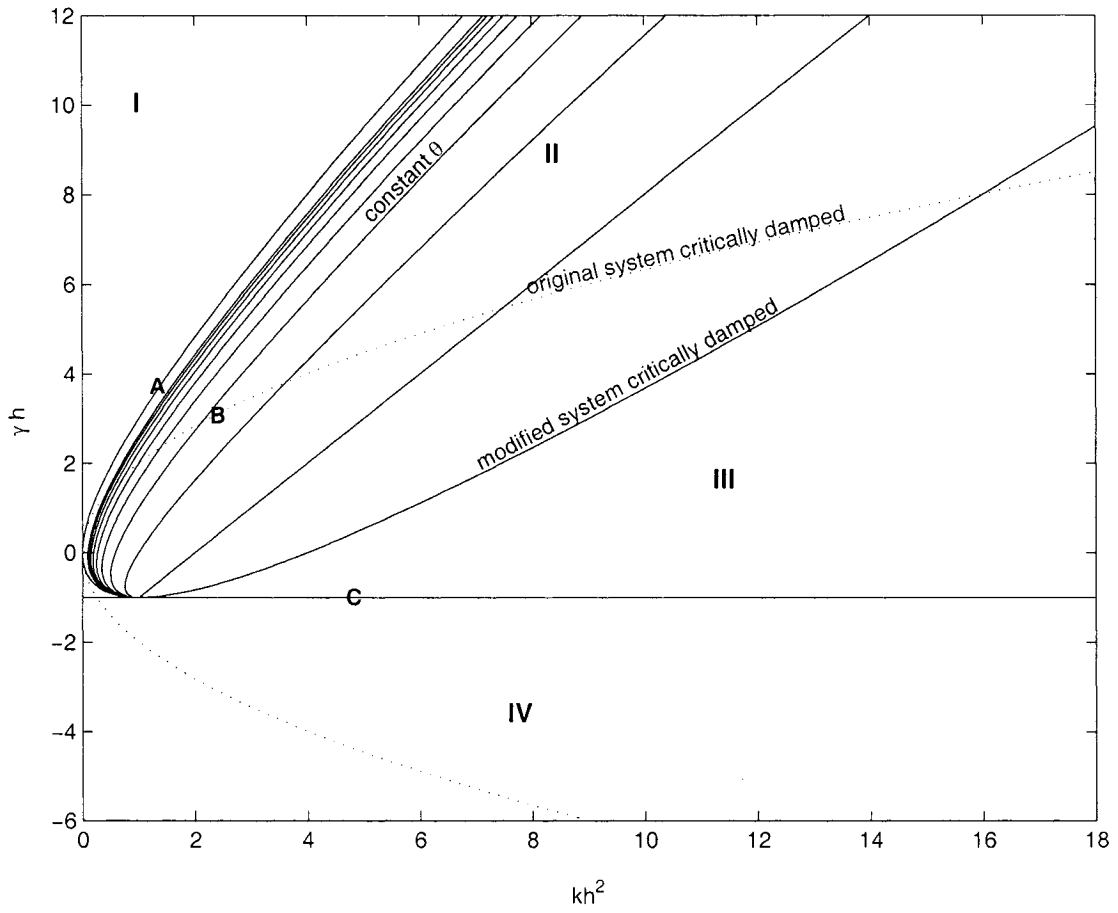


Figure 3.9: Lines of constant θ plotted over the diagram shown in Fig. 2.2. The lines strongly characterize the interesting behaviour of the average change in energy and correspond to the troughs and crests in Fig. 3.10.

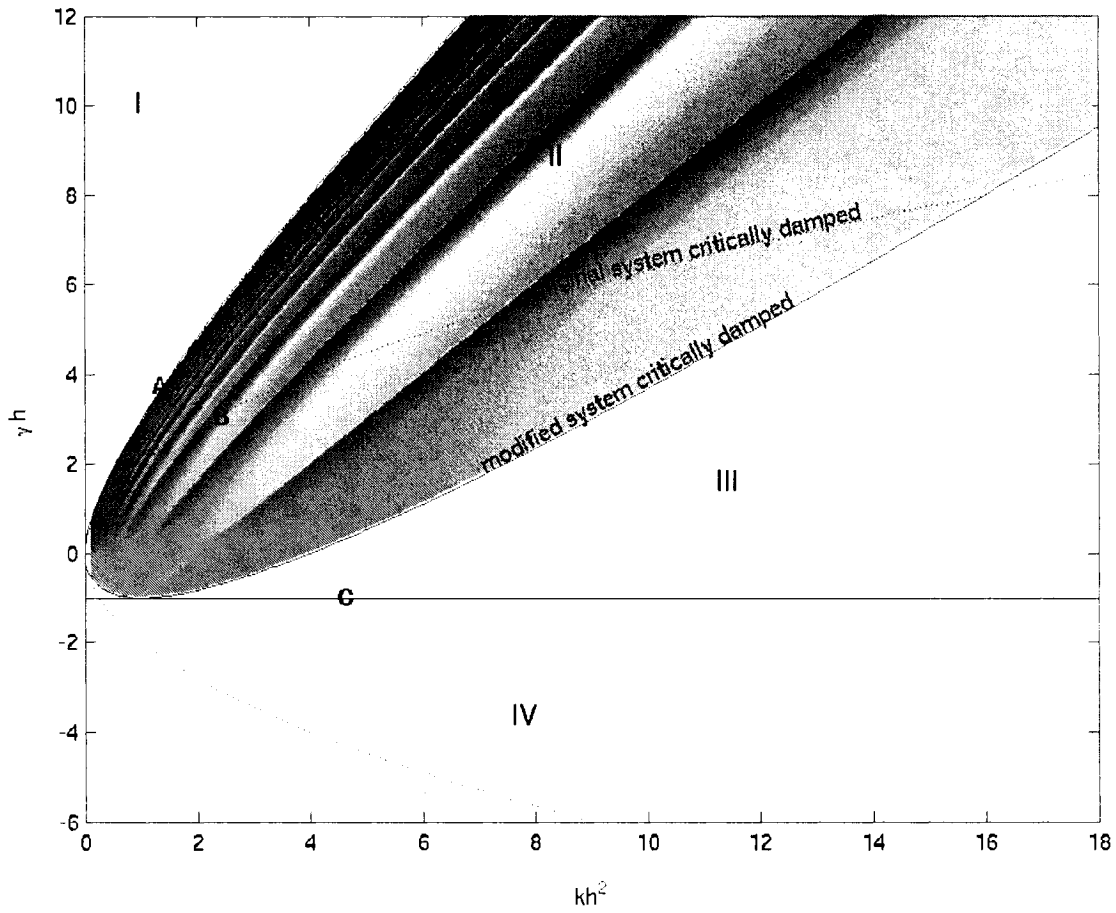


Figure 3.10: Log of the average change in energy in region **II**. The troughs and crests correspond to lines of constant θ (see Fig. 3.9). The average behaviour in region **III** is relatively unremarkable and has been excluded.

Chapter 4

Systems of Particles: Energy Growth in One-Dimensional Systems

We now turn our attention to the numerical integration of dynamical systems within the context of molecular dynamics modeling. Specifically, we consider the problem of the symplectic Euler method (1.5) applied to a system of N particles whose interactions are governed by the pairwise inter-particle potential:

$$V(r) = \begin{cases} \frac{1}{4}k(r-d)^2, & r-d < 0 \\ 0, & r-d \geq 0 \end{cases} \quad (4.1)$$

where r is the distance of separation of the centres of the two particles each of radius d , and k is Young's modulus. In Section 4.1, we apply the results of Chapter 3 regarding energy change due to particle-wall collisions to two-particle collisions, determining the post-collision energy of a two-particle system as a function of the initial (pre-collision) conditions. In Section 4.2, the model system of N interacting particles in one dimension is described. We make a number of assumptions which are appropriate for models of low density systems and derive an estimate of the energy as a function

of time where time is measured in number of collisions. Energy growth predictions are compared with the results of computer simulations.

4.1 Two-particle collisions

Consider a collision between two particles i and j governed by linear restoring and damping forces

$$\begin{cases} \dot{x}_j = v_j \\ \dot{v}_j = -\left(\frac{k}{2}(x_j - x_i - d) + \frac{\gamma}{2}(v_j - v_i)\right) \chi_{\{x_j - x_i - d < 0\}}(x_i, x_j) \\ \dot{x}_i = v_i \\ \dot{v}_i = +\left(\frac{k}{2}(x_j - x_i - d) + \frac{\gamma}{2}(v_j - v_i)\right) \chi_{\{x_j - x_i - d < 0\}}(x_i, x_j) \end{cases} \quad (4.2)$$

where x_i, x_j, v_i and v_j are the positions and velocities of the particles. d is the particle diameter. k and γ are Young's modulus and damping coefficient respectively and χ_A is the characteristic function of the set A . Any two-particle central force problem can be transformed into a one-dimensional problem by a simple change of variables. The reader is referred to Chapter 3 of [17] for a more detailed explanation. Appropriately adding and subtracting the lines of (4.2), we can write the system as

$$\begin{cases} \dot{x}_j - \dot{x}_i = v_j - v_i \\ \dot{v}_j - \dot{v}_i = -(k(x_j - x_i - d) + \gamma(v_j - v_i)) \chi_{\{x_j - x_i - d < 0\}}(x_i, x_j) \\ \dot{x}_i + \dot{x}_j = v_i + v_j \\ \dot{v}_i + \dot{v}_j = 0 \end{cases} \quad (4.3)$$

Substituting $R = \frac{1}{2}(x_i + x_j)$, $r = x_j - x_i$, $v_R = \frac{1}{2}(v_i + v_j)$ and $v_r = v_j - v_i$ in (4.3) we have

$$\begin{cases} \dot{r} = v_r \\ \dot{v}_r = -(k(r - d) + \gamma v_r) \chi_{\{r - d < 0\}}(r) \\ \dot{R} = v_R \\ \dot{v}_R = 0 \end{cases} \quad (4.4)$$

Applying the symplectic Euler method to (4.2) yields a discrete system which may be rewritten using a similar change of variables:

$$\begin{cases} x_j^{n+1} &= x_j^n + hv_j^{n+1} \\ v_j^{n+1} &= v_j^n - \left(\frac{kh}{2}(x_j^n - x_i^n - d) + \frac{\gamma h}{2}(v_j^{n+1} - v_i^{n+1})\right) \chi_{\{x_j^n - x_i^n - d < 0\}}(x_i^n, x_j^n) \\ x_i^{n+1} &= x_i^n + hv_i^{n+1} \\ v_i^{n+1} &= v_i^n + \left(\frac{kh}{2}(x_j^n - x_i^n - d) + \frac{\gamma h}{2}(v_j^{n+1} - v_i^{n+1})\right) \chi_{\{x_j^n - x_i^n - d < 0\}}(x_i^n, x_j^n) \end{cases} \quad (4.5)$$

Adding and subtracting lines of (4.5) in the same way as in (4.3), letting $R^n = \frac{1}{2}(x_i^n + x_j^n)$, $r^n = x_j^n - x_i^n$, $v_R^n = \frac{1}{2}(v_i^n + v_j^n)$ and $v_r^n = v_j^n - v_i^n$ and rearranging we have

$$\begin{cases} v_r^{n+1} &= v_r^n - (kh(r^n - d) + \gamma h v_r^{n+1}) \chi_{\{r^n - d < 0\}}(r^n) \\ r^{n+1} &= r^n + hv_r^{n+1} \\ v_R^{n+1} &= v_R^n \\ R^{n+1} &= R^n + hv_R^{n+1} \end{cases} \quad (4.6)$$

When the particles are colliding, $\chi_{\{r^n - d < 0\}}(r^n) = 1$ and (4.6) may be written more succinctly as

$$\begin{cases} \begin{pmatrix} r^{n+1} \\ v_r^{n+1} \end{pmatrix} &= \frac{1}{1+\gamma h} (\mathbf{I} + \mathbf{A}_h) \begin{pmatrix} r^n \\ v_r^n \end{pmatrix} \\ R^{n+1} &= R^n + hv_R^n \\ v_R^{n+1} &= v_R^n \end{cases} \quad (4.7)$$

Under the given transformations, we see that (4.5) is equivalent to integration of the r , v_r variables via the mapping (2.11) and exact integration of the R , v_R variables. This means that the predictions for the post-collision velocity presented in Chapter 3 for particle-wall collisions may be applied to predict the post-collision relative velocity for two-particle collisions. Given the initial (pre-collision) conditions, the post-collision relative velocity will be given by the square-root of (3.11). Reverting back to the

original variables we then have the system

$$\begin{cases} v_j^f - v_i^f &= \sqrt{\frac{E_f}{E_0}(\mu, kh^2, \gamma h)}(v_i^0 - v_j^0) \\ v_j^f + v_i^f &= v_i^0 + v_j^0 \end{cases} \quad (4.8)$$

where v^f and v^0 indicate post- and pre-collision values respectively. Solving this system for the total energy of the particles yields

$$E_{ij}^f = \frac{1}{2} \left(1 + \frac{E_f}{E_0}(\mu, kh^2, \gamma h) \right) E_{ij}^0 + \frac{1}{2} \left(1 - \frac{E_f}{E_0}(\mu, kh^2, \gamma h) \right) v_i^0 v_j^0. \quad (4.9)$$

where $E_{ij}^0 = (v_i^0)^2 + (v_j^0)^2$ and $E_{ij}^f = (v_i^f)^2 + (v_j^f)^2$. If $\gamma = 0$ and $\theta = \frac{\pi}{m}$, $m = 1, 2, \dots$, then $\frac{E_f}{E_0} = 1$, and the energy of each particle is conserved across the collision.

4.2 Systems of particles

In molecular dynamics, mathematically deterministic systems are often treated as stochastic, at least in terms of certain macroscopic quantities, such as energy or temperature. The deterministic trajectories are supposed to approximate some stochastic process in the distribution sense. Usually these systems are assumed to uphold some form of ergodicity with respect to a particular state (statistical) variable. Important to this assumption is that the number of particles is large and that the phase space is sampled quickly by the system. Taking the number of particles to be large allows assumptions regarding the independence of particles and ensures that thermodynamic quantities such as temperature are well defined and make sense. In setting up these models, it is often useful to assume the times between collisions to be identically distributed random variables with a particular distribution. It is shown in [46] that assuming a particular distribution is not necessary as the time between collisions converges weakly with the number of particles to an exponential random variable. If the system is ergodic or in some sense “nearly ergodic” over the time intervals of simulations run on the computer, the underlying random process can be observed

and the statistics of the simulation will well approximate those of the underlying stochastic system. For discussion and analysis of stochastic dynamics approximated by deterministic (and random) dynamical systems see [57], [47], [53], [54] and [55]. Freidmann [16] also briefly considers the introduction of stochasticity by numerical methods.

Here we consider systems of N particles on a periodic linear domain of length L interacting via the local pairwise linear restoring force described in Chapter 3. The results for two-particle collisions are applied to describe the evolution of the statistics of the total energy of the system and of the particle velocities.

4.2.1 Consideration of dimension

Systems of interacting particles in one dimension will not in general be chaotic or ergodic and may even display neutrally stable orbits. Nonetheless, given suitable initial conditions (Boltzmann distribution) and a large number of particles, non-ergodic and especially periodic behaviour will not be apparent. In this case, velocity statistics of the one-dimensional system may be reasonably modeled by a stochastic process over finite time intervals.

4.2.2 Energy growth for 1-d system

Consider a simulation of a system of N particles in one dimension which interact pairwise via the linear restoring force (plus damping) with the symplectic Euler method. Since changes in velocities occur only through collisions, it is natural to measure time in discrete increments of collisions, thus eliminating the problem of estimating collision rates. In real systems, measuring time in this way is not always possible and it will be desirable to have an understanding of the collision rates and their relation to the total energy of the system. The problem of determining the distribution of

collision times in this context is treated in Chapter 5 of [46].

Define

1. The velocity of the particle i after the n th collision: v_i^n .
2. The total energy of the system after the n th collision:

$$E^n = \sum_{i=1}^N (v_i^n)^2. \quad (4.10)$$

3. The energy of particle k after the n th collision:

$$E_k^n = (v_k^n)^2. \quad (4.11)$$

4. The energy of two particles i and j after the n th collision:

$$E_{ij}^n = (v_i^n)^2 + (v_j^n)^2. \quad (4.12)$$

A number of assumptions are made.

1. Collisions involving three or more particles are rare.
2. Velocities of non-colliding particles are constant in time.
3. Velocities are *iid* with Boltzmann Distribution

$$P(v_i \in [\nu_i, \nu_i + d\nu]) = f(\nu_i)d\nu = \frac{1}{\sqrt{2\pi\sigma_n^2}} e^{-\frac{\nu_i^2}{2\sigma_n^2}} d\nu. \quad (4.13)$$

4. Only one collision happens at a time.

5. Positions of colliding particles are independent of their velocities (i.e. μ is independent of $v_i, i = 1, \dots, N$).

An important implication of Assumption 3 is that the collisions change the velocities slowly so that the system is at all times near equilibrium and satisfies the thermodynamic relation

$$\frac{\langle E^n \rangle}{N} = \sigma_n^2. \quad (4.14)$$

This also implies that energy is on average distributed uniformly over the system: $\langle E_i^n \rangle = \frac{1}{N} \langle E^n \rangle$ at all moments in time. Over long time intervals, the random forcing introduced by the method at each collision may in fact shift the system away from the Boltzmann equilibrium distribution. This is the kind of problem one might encounter in Dissipative Particle Dynamics (Molecular Dynamics with random and deterministic damping and forcing terms), where one attempts to mitigate problems with shifted equilibrium distributions by choosing the damping and random forcing parameters carefully [15]. In the problem presented here, however, the random forcing is an artifact of the numerically integrated collision and is not given by a “tunable” random term in the interparticle potential. Assumption 5 allows us to independently take expectations over μ , which parameterizes the initial conditions of a collision (see Section 3.1), and over v_i and v_j , the velocities of the colliding particles.

Now suppose the $(n + 1)$ th collision involves particles i, j and that no other collisions occur at the same time. The energy of the system just after this collision is

given by

$$\begin{aligned}
E^{n+1} &= \sum_{k \neq i, j}^N E_k^{n+1} + E_{ij}^{n+1} \\
&= \sum_{k \neq i, j}^N E_k^n + \frac{1}{2} \left(1 + \frac{E_f}{E_0}(\mu_n, kh^2, \gamma h) \right) E_{ij}^n + \frac{1}{2} \left(1 - \frac{E_f}{E_0}(\mu_n, kh^2, \gamma h) \right) v_i^n v_j^n \\
&= E^n - \frac{1}{2} \left(1 - \frac{E_f}{E_0}(\mu_n, kh^2, \gamma h) \right) E_{ij}^n + \frac{1}{2} \left(1 - \frac{E_f}{E_0}(\mu_n, kh^2, \gamma h) \right) v_i^n v_j^n. \quad (4.15)
\end{aligned}$$

using (4.9) and the fact that the energies of the non-colliding particles are unchanged. Thus we have a stochastic mapping for the particle velocities with random parameter μ . Taking averages over μ_n and $\nu = (\nu_1, \dots, \nu_N)$ yields

$$\langle E^{n+1} \rangle_{\mu_n, \nu} = \langle E^n \rangle_{\mu_n, \nu} + \frac{1}{2} \left(1 - \langle \frac{E_f}{E_0} \rangle_{\mu_n} \right) (\langle v_i^n v_j^n \rangle_{\nu_i, \nu_j} - \langle E_{ij}^n \rangle_{\nu_i, \nu_j}) \quad (4.16)$$

From here on, we will simply write $\langle E^n \rangle = \langle E^n \rangle_{\nu_i, \nu_j}$ and $\langle \frac{E_f}{E_0} \rangle = \langle \frac{E_f}{E_0} \rangle_{\mu_n}$.

Though we have that the μ_n are *iid* uniformly distributed on $[0, 1)$, to write (4.16) as an expression involving state variables alone (i.e. the average energy or temperature) we need to compute expectations over the velocities of the colliding particles v_i, v_j . The joint probability distribution function of the velocities v_i, v_j must be determined in order that the expectations in (4.16) can be written explicitly in terms of $\langle E^n \rangle$ and σ^2 . The approach followed here is that presented in [46] for hard spheres or billiards where a rigorous derivation of the joint pdf can be found. There, a conditional pdf is derived and used to obtain an expression for the average rate of collisions between a given particle of velocity u and all particles with velocity v . Though billiard systems involve instantaneous collisions and can not be exactly represented by a system of differential equations, it is shown in [54] that the non-differentiable flow of the hard-sphere system can be approximated by the soft-sphere model in the limit as the spring constant k goes to infinity.

The first key observation to make is to notice that for conservative billiard systems, where when particles collide they simply exchange velocities instantaneously, we can

think of the particles as point particles (with zero radius) on a reduced interval of length $L - dN$, where L is the length of the domain, d is the diameter of the particles and N the number of particles. Furthermore, since the collisions are instantaneous, the particles can be thought of as not colliding but passing through one another. The pdf $f(\nu)$ is the rate of occurrence or likelihood of particles with velocity $v = \nu$. The rate of occurrence of pairs of particles with velocities $v_i = \nu_i$ and $v_j = \nu_j$ is proportional to the product $f(\nu_i)f(\nu_j)$. Given a pair of particles with the above velocities situated in a periodic domain, the particles will cross each other (collide) with a frequency proportional to their relative velocity, $|\nu_i - \nu_j|$. So it seems plausible that the collision rate for particles of velocities $v_i = \nu_i$ and $v_j = \nu_j$ is proportional to $f(\nu_i)f(\nu_j)|\nu_i - \nu_j|$. As stated in [46], the joint pdf is given by the fraction of collisions between particles with velocities ν_i and ν_j to collisions between all particles:

$$f(\nu_i, \nu_j) = \frac{f(\nu_i)f(\nu_j)|\nu_i - \nu_j|}{\int \int f(u)f(v)|u - v|dudv}. \quad (4.17)$$

This conservative billiard system derivation does not account for the fact that collisions are not only soft but non-conservative. This simple model does, however, provide reasonable results and opens the door to further analysis involving non-conservative billiard systems.

Having now obtained an expression for the joint pdf of the velocities of colliding particles, we can compute the expectations in (4.16). A few lines in any symbolic computation package yield:

$$f(\nu_i, \nu_j) = \frac{1}{4\sqrt{\pi}\sigma^3}f(\nu_i)f(\nu_j)|\nu_i - \nu_j|$$

$$\langle E_{ij}^n \rangle = \int \int (\nu_i^2 + \nu_j^2)f(\nu_i, \nu_j)d\nu_id\nu_j = 3\sigma_n^2 \quad (4.18)$$

$$\langle v_i^n v_j^n \rangle = \int \int \nu_i \nu_j f(\nu_i, \nu_j)d\nu_id\nu_j = -\frac{\sigma_n^2}{2} \quad (4.19)$$

Inserting these expressions into (4.16), substituting $\sigma_n^2 = \langle E^n \rangle / N$ using (4.14) and rearranging gives a nice expression for the growth of the expected energy of the

system

$$\begin{aligned}\langle E^{n+1} \rangle &= \left[1 + \frac{7}{4} \frac{1}{N} \left(\langle \frac{E_f}{E_0} \rangle - 1 \right) \right] \langle E^n \rangle \\ \Rightarrow \langle E^n \rangle &= \left[1 + \frac{7}{4} \frac{1}{N} \left(\langle \frac{E_f}{E_0} \rangle - 1 \right) \right]^n \langle E^0 \rangle.\end{aligned}\quad (4.20)$$

The expected energy of the system grows exponentially with the number of collisions. Results from a single run of 1000 particles over 130 000 collisions are shown in Fig. 4.1. The velocity histograms (Top), show a slight broadening of what looks to be a roughly Gaussian distribution. However, much longer runs with more particles are needed to further investigate the change in the distribution of velocities. In all simulations presented here, the damping parameter γ is zero. What is plotted as points in Fig. 4.2, 4.3, 4.4 and 4.5 is the mean and mean \pm one standard deviation of the energy relative to initial energy calculated from a set of 200 computer simulations for each of the parameter combinations. The solid lines in these figures represent the mean energy relative to initial energy as predicted by the model in (4.20).

In Fig. 4.2, a comparison of the theoretical energy predictions and energy statistics from three series of 200 simulations, each is shown for three different values of the number of particles. All other system parameters are the same for each trial. The poorer fit between model and simulations for the smaller number of particles suggests that finite system size becomes important as the ratio of the number of collisions (the duration of the simulation) to the number of particles grows. However, even if we compare the run of 500 particles at the 500th collision to the run of 1000 particles at the 1000th collision, it seems that the model more accurately captures the energy growth of the system with more particles.

Fig. 4.3 shows energy predictions of the model and energy statistics from simulations as a function of number of collisions for four values of the density, ρ , while all other system parameters are fixed. It is to be expected that as the density increases, Assumptions 1 and 4 will no longer be valid and the theoretical model will less accu-

rately capture energy growth in the simulation. In particular, three particle collisions can no longer be considered to be negligible especially in the time-discretized system where particles do not interact as perfect billiards but experience collisions which are not instantaneous.

The effect of varying the parameter kh^2 and the variance of the velocity distribution, σ^2 , is shown respectively in Figs. 4.4 and 4.5. Again, all other system parameters are the same over each trial. The quality of the fit between model and simulation statistics seems largely unaffected by changes in kh^2 . Changing σ^2 amounts to changing the initial temperature of the system and involves merely varying the distribution of initial velocities. In both the simulation statistics and in the model, very little difference is seen over the range of values of σ^2 shown in Fig. 4.5.

In the final plot, Fig. 4.6, the energies of four simulations of 100 particles are shown over a period of 100000 collisions. The value of kh^2 is different for each of the four simulations and is chosen so that the energy is exactly preserved over two-particle collisions. It is notable that the only simulation with no obvious drift in energy over the 100000 collisions is the case where $kh^2 = 2$ – the simulation with the largest time step. This is likely due to a higher frequency of occurrence of multi-particle collisions in the simulations with smaller time steps. In these simulations, kh^2 is varied by changing k while holding h constant. For $kh^2 = 2$, collisions last *exactly* one time step but for the other cases collisions have a duration of 2 time steps or more. Since h is the same for the four simulations, the number of time steps between collisions remains roughly the same, however the duration of collisions is longer for smaller values of kh^2 and there is a greater “chance” for multi-particle collisions to occur.

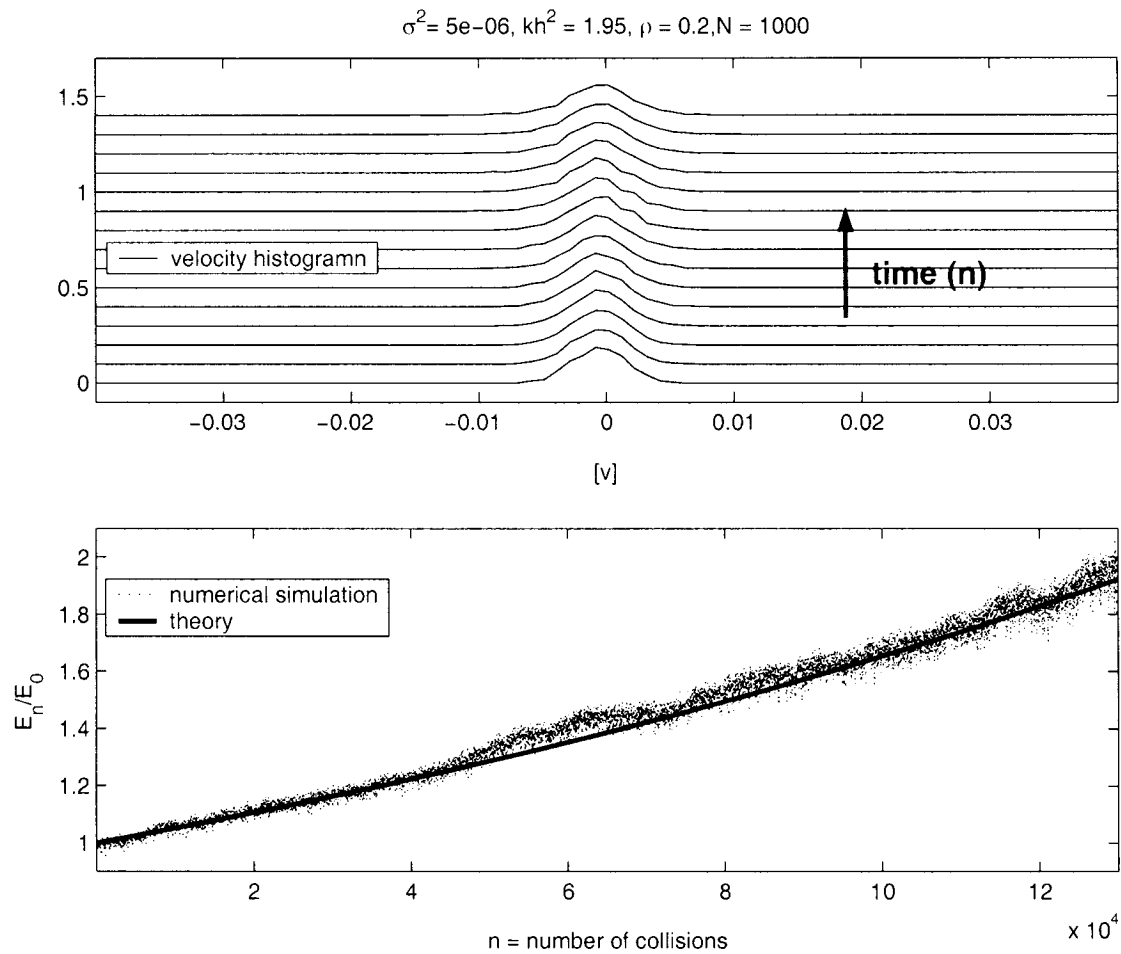


Figure 4.1: Particle velocities are recorded from a single simulation of 1000 particles in one dimension over a period of 130 000 collisions. Top: Velocity histograms are plotted at regular intervals. The plots are vertically shifted for visibility. Bottom: Energy growth, relative to the initial energy of the system, is plotted as a function of the number of collisions. Simulation energy is plotted as points and the theoretical prediction is the solid line.

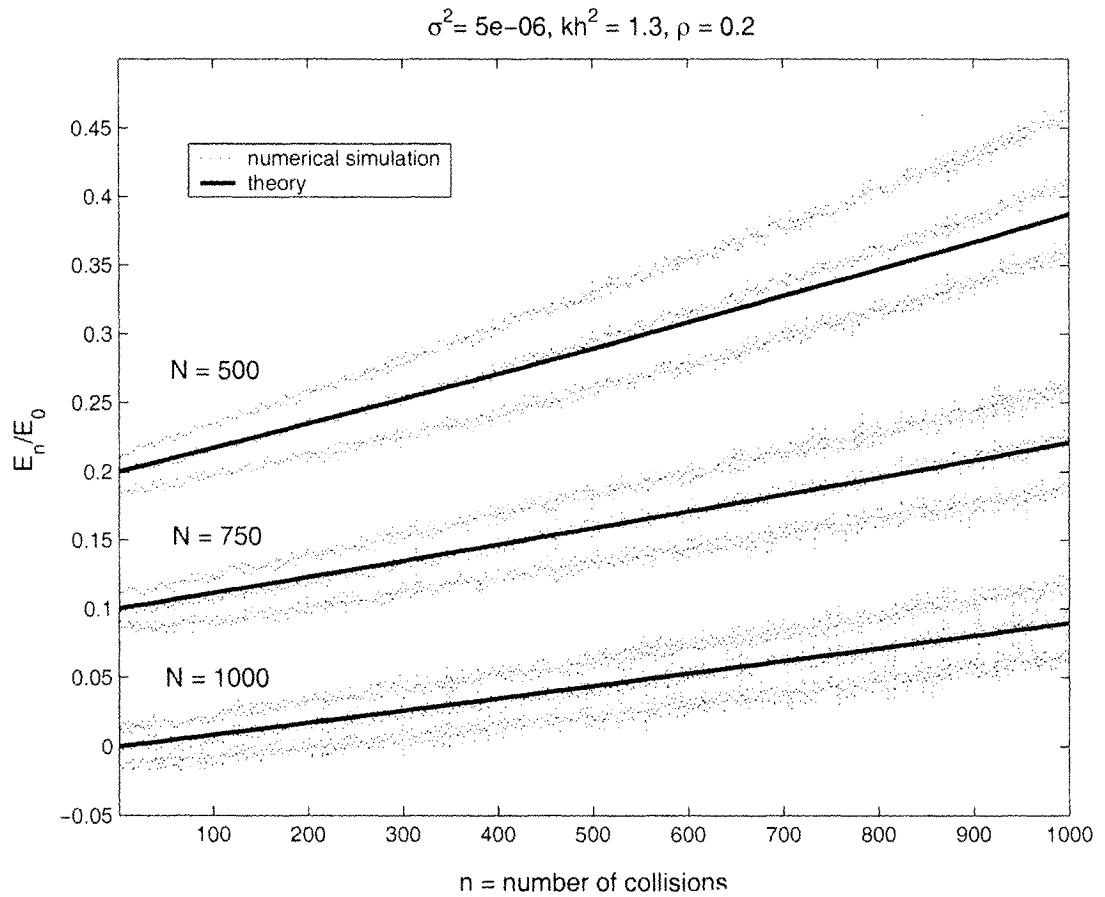


Figure 4.2: Energy statistics are presented from three series of 200 simulations, each run over a period of 1000 collisions. Average energy and energy ± 1 standard deviation, relative to initial energy, are plotted (dotted line) with the theoretical prediction of the expected value of energy (solid line) for runs with 500, 750 and 1000 particles. Here and in following plots, all averages pass through (0, 1) but are shifted vertically for visibility.

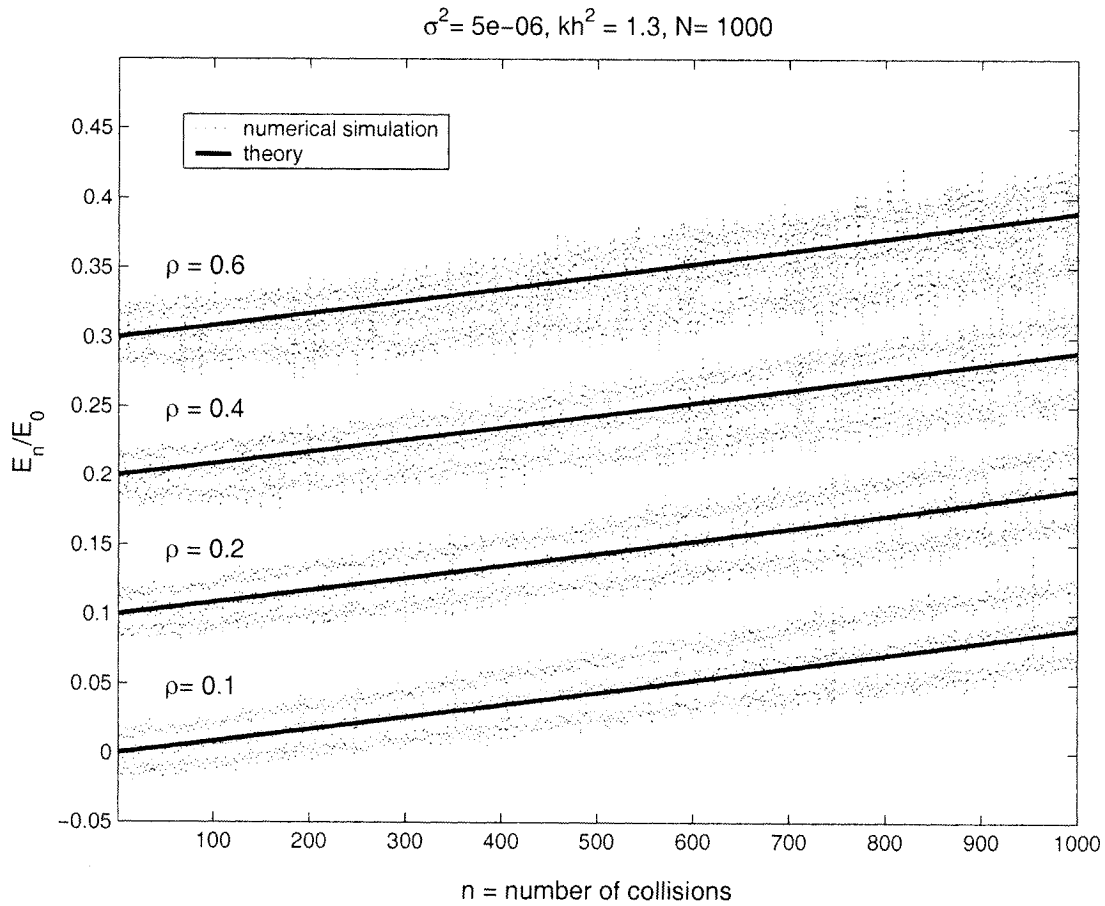


Figure 4.3: Energy statistics are presented from four series of 200 simulations, each run over a period of 1000 collisions. Average energy and energy ± 1 standard deviation, relative to initial energy, are plotted (dotted line) with the theoretical prediction of the expected value of energy (solid line) for runs with $\rho = 0.1, 0.2, 0.4, 0.6$. Lines are vertically shifted for visibility.

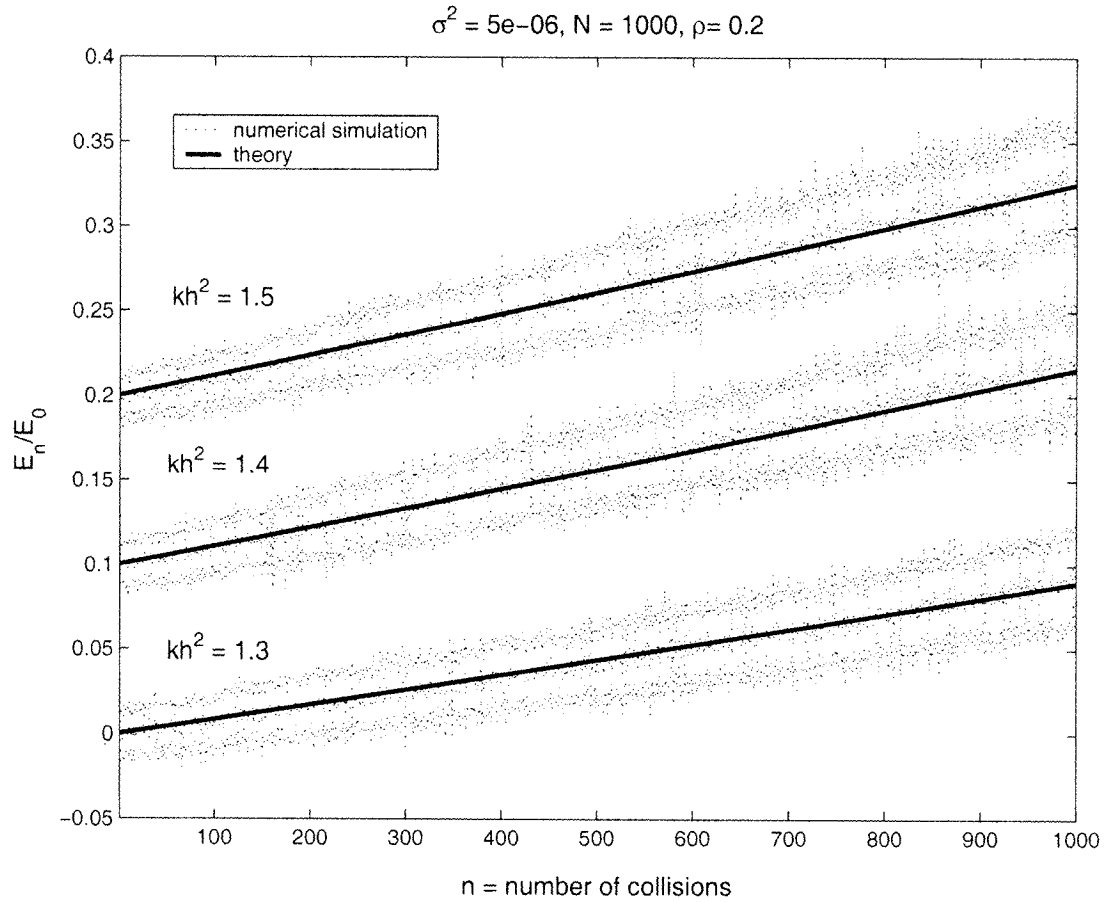


Figure 4.4: Energy statistics are presented from three series of 200 simulations, each run over a period of 1000 collisions. Average energy and energy ± 1 standard deviation, relative to initial energy, are plotted (dotted line) with the theoretical prediction of the expected value of energy (solid line) for runs with $kh^2 = 1.3, 1.4, 1.5$. Lines are vertically shifted for visibility.

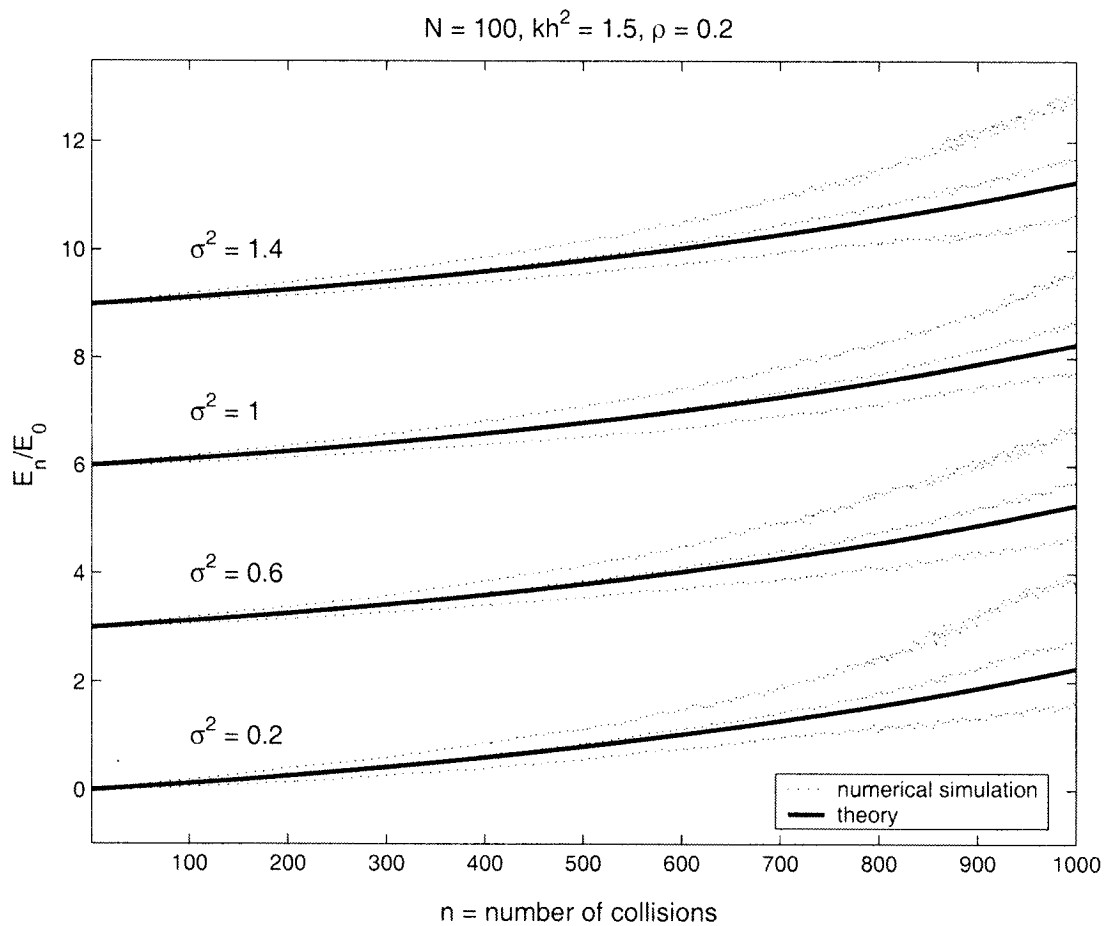


Figure 4.5: Energy statistics are presented from four series of 200 simulations, each run over a period of 1000 collisions. Average energy and energy ± 1 standard deviation, relative to initial energy, are plotted (dotted line) with the theoretical prediction of the expected value of energy (solid line) for runs with $\tau = 0.2, 0.6, 1.0, 1.4$. Lines are vertically shifted for visibility.

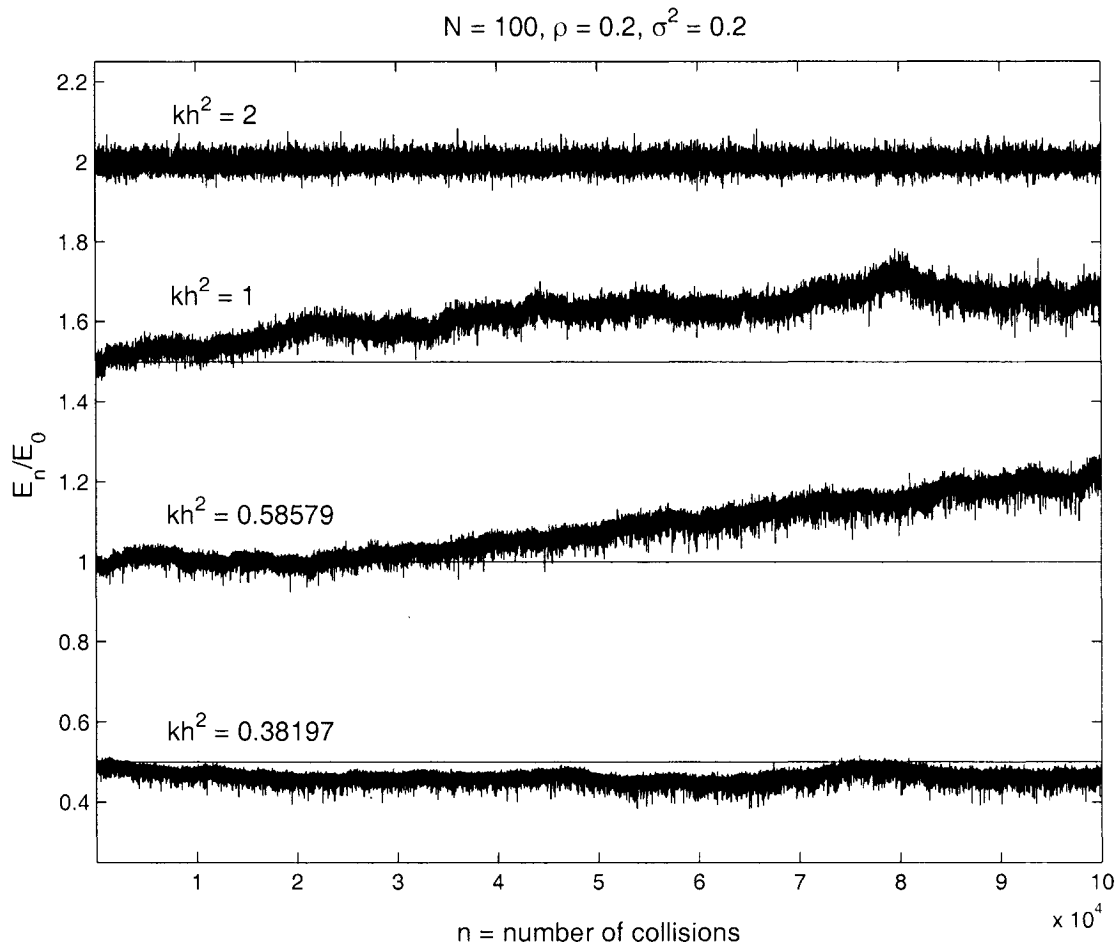


Figure 4.6: Energy, relative to initial energy, of systems of 100 particles in one dimension. The values of kh^2 were chosen so that $\theta = \frac{\pi}{m}$, $m = 1, 2, 3, 4$ and the energy is conserved across two-particle collisions. In the lower three plots, the slow drift in energy is likely due to the non-negligible presence of multi-particle collisions when two-particle collisions last longer than one time step. Lines are vertically shifted for visibility.

Conclusion

It has been shown here that for numerically integrated systems of locally interacting particles, the numerical method can introduce errors in a systematic and statistically predictable way. Computations involving pairwise interacting particle systems with a linear-spring Hamiltonian integrated using the symplectic Euler method exhibit such a predictable growth in energy.

Backward error analysis and the method of modified equations provide a means of obtaining analytic expressions to predict error introduced during collisions by the numerical integrator and the discretization of time. It is important to note, however, that it is equally feasible to analyze the collisions without ever resorting to backward error analysis. One may compute the outgoing velocity as a function of the initial conditions and use this information to make (approximate) statistical predictions about the energy growth of the system. This approach would be germane for nearly all other types of collisions where the modified system is not linear and the *exact* modified equation does not exist in the sense of convergence of the series (2.5). Furthermore, in many cases the expectations taken with respect to the randomly distributed initial conditions will often involve integrals which can only be evaluated using quadrature.

There are a number of areas into which future work might proceed. It seems quite possible to extend this analysis to systems of particles in higher dimensions as well as to those involving other two-body potentials – such as the commonly used Lennard-Jones potential. Simulations run over much longer periods of time with

many more particles would provide useful information regarding the evolution of the velocity probability distribution function. In contrast to the purely investigative focus of the present work, new methods might be constructed which embody the dynamics of the discretized collisions and more accurately represent the desired dynamics. In particular, the addition of a post-collision correction, either as a deterministic quantity or as a appropriately chosen randomly distributed variable (or both), may provide a new method with improved behaviour for the given system. This kind of corrective tuning would be along the lines of a Dissipative Particle Dynamics approach [15] though the analysis presented here provides a means of justifying the addition of non-Gaussian random dissipation or forcing to collision forces.

The analysis shown here will in many cases be too involved for systems involving many different kinds of particles or those involving asymmetric particles. Nonetheless, these simple systems do offer some qualitative insight into the range of behaviour of numerically integrated particle systems.

Appendix A

Glossary of symbols

1. k - Young's modulus (spring constant over mass)
2. γ - viscosity over mass
3. h - time step of the numerical method
4. θ - argument of the complex eigenvalues of the numerical map (2.11)
5. \mathbf{A} - linear operator of the linearized damped harmonic oscillator system (2.9)
6. \mathbf{A}_h - see (2.11)
7. $\tilde{\mathbf{A}}_h$ - modified linear operator (see (2.12))
8. λ_{\pm} - eigenvalues of \mathbf{A}
9. $\lambda_{h\pm}$ - eigenvalues of \mathbf{A}_h
10. $\tilde{\lambda}_{h\pm}$ - eigenvalues of $\tilde{\mathbf{A}}_h$
11. $y = (x, v)^T$ - exact solution of (2.9)
12. $y_n = (x_n, v_n)^T$ - numerical solution given by (2.11)

13. $\tilde{y} = (\tilde{x}, \tilde{v})^T$ - exact modified solutions (solutions of (2.12))
14. \mathcal{H} - Hamiltonian of (undamped) harmonic oscillator
15. $\tilde{\mathcal{H}}_h$ - modified Hamiltonian
16. \tilde{T} - period of the modified system
17. **A,B,C,I,II,III,IV** - curves and regions described in Fig. 2.2
18. μ - parameterizes the initial conditions of a collision (see Fig. 3.1)
19. μ' - see Fig. 3.2
20. ν - vector of particle velocities
21. ρ - linear density of system of particles
22. σ^2 - variance of the distribution of initial velocities ($\frac{1}{2}k_B * \text{temperature}$)
23. d - diameter of particles
24. r - distance between centres of two colliding particles
25. R - centre of mass of two colliding particles

Bibliography

- [1] M. O. Ahmed and R. M. Corless. The method of modified equations in Maple. In M. Wester and S. Steinberg, editors. *Electronic Proceedings of the 3rd International IMACS Conference on Applications of Computer Algebra*, 1997.
- [2] E. Barth and B. Leimkuhler. Symplectic methods for conservative multibody systems. In G. Patrick, editor. *Proceeding of the workshop on symplectic integration algorithms*. Fields institute, 1993.
- [3] G. Benettin and A. Giorgilli. On the Hamiltonian interpolation of near-to-the-identity symplectic mappings with application to symplectic integration algorithms. *Journal of Statistical Physics*, 74(5/6):1117-1142, 1993.
- [4] W.-J. Beyn. *Advances in Numerical Analysis*, volume 1, chapter Numerical methods for dynamical systems, pages 175-236. Oxford Science Publications, 1991.
- [5] J. Candy and W. Rozmus. A symplectic integration algorithm for separable Hamiltonian functions. *Journal of Computational Physics*, 92:230-256, 1989.
- [6] P. J. Channell. Symplectic integration algorithms. *Los Alamos National Laboratory Report*, Report AT-6ATN 83-9, 1983.
- [7] P. J. Channell and C. Scovel. Symplectic integration of Hamiltonian systems. *Nonlinearity*, 3:231-259, 1990.

- [8] R. M. Corless. Error backwards. *Contemporary Mathematics*, 172:31–62, 1994.
- [9] B. J. Daly. The stability properties of a coupled pair of nonlinear partial differential equations. *Math. Comput.*, 17:346–360, 1963.
- [10] R. DeVogelaere. Methods of integration which preserve the contact transformation property of the Hamiltonian equations. *Department of Mathematics, University of Notre Dame Report*, 4, 1956.
- [11] D. J. D. Earn and S. Tremaine. Exact numerical studies of Hamiltonian maps: iterating without roundoff error. *Physica D*, 56:1–22, 1992.
- [12] T. Eirola. Aspects of backward error analysis of numerical ode's. *J. of Comp. and Applied Mathematics*, 45:65–73, 1993.
- [13] K. Feng. On difference schemes and symplectic geometry. *J. Comput. Math.*, 4:279–289, 1986.
- [14] K. Feng. Formal power series and numerical algorithms for dynamical systems. In *Proceedings of international conference on scientific computation*, pages 28–35, 1991.
- [15] D. Frenkel and B. Smit. *Understanding molecular simulation from algorithms to applications*. Elsevier Academic Press, San Diego, 2002.
- [16] A. Friedman. Numerically induced stochasticity. *Nuclear Physics B (Proc. Suppl.)*, 2:599–600, 1987.
- [17] H. Goldstein. *Classical Mechanics*. Addison-Wesley Press, Inc., 1951.
- [18] O. Gonzalez, D. J. Higham, and A. M. Stuart. Qualitative properties of modified equations. *J. of Numerical Analysis*, 19:169–190, 1999.

- [19] D. F. Griffiths and J. M. Sanz-Serna. On the scope of the method of modified equations. *J. Sci. Statist. Comput.*, 7:994–1008, 1986.
- [20] E. Hairer. Backward analysis of numerical integrators and symplectic methods. *Annals of numerical mathematics*, 1:107–132, 1994.
- [21] E. Hairer and P. Leone. Order barriers for symplectic multi-value methods. In D. F. Griffiths, D. J. Higham, and G. Watson, editors, *Numerical Analysis 1997. Proceedings of the 17th Dundee biannual Conference, Pitman Research Notes in Mathematics series*, volume 380, pages 133–149, 1998.
- [22] E. Hairer and C. Lubich. The life-span of backward error analysis for numerical integrators. *Numerische Mathematik*, 76:441–462, 1997.
- [23] E. Hairer and C. Lubich. Asymptotic expansions and backward analysis for numerical integrators. In *Dynamics of Algorithms (Minneapolis, MN, 1997), IMA VOL. Math. Appl. 118*, pages 91–106. Springer, New York, 2000.
- [24] E. Hairer, C. Lubich, and G. Wanner. *Geometric Numerical Integration – Structure-Preserving Algorithms for Ordinary Differential Equations*. Springer-Verlag, New York, 2002.
- [25] E. Hairer, C. Lubich, and G. Wanner. Geometric numerical integration illustrated by the Störmer-Verlet method. *Acta numerica*, pages 339–450, 2003.
- [26] E. Hairer and D. Stoffer. Reversible long-term integration with variable step-sizes. *SIAM J. Sci. Comput.*, 18:257–269, 1997.
- [27] E. Hairer and G. Wanner. On the butcher group and general multivalued methods. *Computing*, 13:1–15, 1974.
- [28] N. J. Higham. *Accuracy and stability of numerical algorithms*. SIAM, Philadelphia, 1996.

- [29] C. W. Hirt. Heuristic stability theory for finite difference equations. *J. Comput. Phys.*, 2:339–355. 1968.
- [30] G. Labelle. Sur l'inversion et l'itération continue des séries formelles. *Europ. J. Combinatorics*, 1:113–138. 1980.
- [31] J. Lambert. *Numerical Methods for Ordinary Differential Systems*. John Wiley & Sons, New York, 1991.
- [32] F. Lasagni. Canonical Runge-Kutta methods. *ZAMP*, 39:952–953. 1988.
- [33] R. I. McLachlan and P. Atela. The accuracy of symplectic integrators. *Nonlinearity*, 5:541–562. 1992.
- [34] R. I. McLachlan and C. Scovel. A survey of open problems in symplectic integration. *Fields Inst. Commun.*, 1998.
- [35] B. Mehlig, D. W. Heermann, and B. M. Forrest. Hybrid monte carlo method for condensed-matter systems. *Phys. Rev. B*, 45:679–685. 1992.
- [36] C. R. Menyuk. Some properties of the discrete Hamiltonian method. *Physica D*, 11:109–129. 1984.
- [37] J. Moser. Lectures on Hamiltonian systems. *Mem. Am. Math. Soc.*, 81:1–60. 1968.
- [38] A. I. Neishtadt. The separation of motions in systems with rapidly rotating phase. *J. Appl. Math. Mech.*, 48:133–139. 1984.
- [39] W. G. Noh and M. H. Protter. Difference methods and the equations of hydrodynamics. *J. Math. Mech.*, 12, 1963.
- [40] S. Reich. *Dynamical systems, numerical integration, and exponentially small estimates*. Habilitationsschrift. Berlin, 1997.

- [41] S. Reich. Backward error analysis for numerical integrators. *SIAM J. Numer. Anal.*, 36(1):1549-1570, 1999.
- [42] R. D. Ruth. A canonical integration technique. *IEEE Trans. Nucl. Sci.*, 30:2669-2671, 1983.
- [43] J. M. Sanz-Serna. *Advances in numerical analysis*, chapter Two topics in non-linear stability. Clarendon Press, Oxford, 1991.
- [44] J. M. Sanz-Serna. Symplectic integrators for Hamiltonian problems: an overview. *Acta Numerica*, 1:243-286, 1991.
- [45] C. Scovel. On symplectic lattice maps. *Physics Letters A*, 159:396-400, 1991.
- [46] H. Sigurgeirsson. *Particle-field models: algorithms and applications*. PhD thesis. Stanford University, 2001.
- [47] H. Sigurgeirsson and A. M. Stuart. Statistics from computations. In *Foundations of Computational Mathematics (Oxford 1999)*, *London Math. Soc. Lecture Note Ser.* 284, pages 323-344. Cambridge University Press, Cambridge, 2001.
- [48] J. C. Simo and N. Tarnow. The discrete energy-momentum method. Conserving algorithms for nonlinear elastodynamics. *ZAMP*, 43:757-792, 1992.
- [49] R. D. Skeel. Symplectic integration with floating-point arithmetic and other approximations. *Applied Numerical Mathematics*, 29:3-18, 1999.
- [50] R. D. Skeel, D. I. Okunbor, and D. J. Hardy. Symplectic variable stepsize integration for n-body problems. *Applied Numerical Mathematics*, 29:19-30, 1999.
- [51] Y. B. Suris. Integrable mappings of the standard type. *Funct. Anal. Appl.*, 23(1):74-75, 1989.

- [52] Y. F. Tang. The symplecticity of multi-step methods. *Computers Math. Applic.*, 25:83–90, 1993.
- [53] P. F. Tupper. Computing statistics for Hamiltonian systems: A case study. Derived from a chapter of Ph.D. thesis, 2002.
- [54] P. F. Tupper. The motion of a tracer particle in a one-dimensional system: analysis and simulation. 2002.
- [55] P. F. Tupper. A test problem for molecular dynamics integrators. 2003.
- [56] A. M. Turing. Rounding-off errors in matrix processes. *Quart. J. Mech. Appl. Math.*, 1:287–308, 1948.
- [57] M. Viana. Stochastic dynamics of deterministic systems. *Instituto de Matematica Pura e Aplicada (IMPA), Rio de Janeiro*. 1997.
- [58] J. von Neumann and H. H. Goldstine. Numerical inverting of matrices of high order. *Bull. Amer. Math. Soc.*, 53:1021–1099, 1947.
- [59] H. Weyl. *The Classical groups*. Princeton Univ. Press, Princeton, 1939.
- [60] J. H. Wilkinson. Error analysis of direct methods of matrix inversion. *J. Assoc. Comput. Mach.*, 8:281–330, 1961.
- [61] J. H. Wilkinson. *Rounding Errors in Algebraic processes*. Prentice-Hall, New Jersey, 1963.
- [62] J. H. Wilkinson. *The algebraic eigenvalue problem*. Oxford University Press, 1965.
- [63] N. N. Yanenko and Y. I. Shokin. First differential approximation method and approximate viscosity of difference schemes. *Phys. Fluids*, 12 (Suppl.):28–33, 1969.

- [64] H. Yoshida. Recent progress in the theory and application of symplectic integrators. *Celestial mechanics and dynamical astronomy*, 56:27-43, 1993.
- [65] G. Zhong and J. E. Marsden. Lie-poisson Hamilton-Jacobi theory and Lie-poisson integrators. *Phys. Lett. A*, 133(3):134-139, 1988.